The Constitutive Function of Native TRPC3 Channels Modulates Vascular Cell Adhesion Molecule-1 Expression in Coronary Endothelial Cells Through Nuclear Factor κB Signaling

Kathryn Smedlund, Jean-Yves Tano and Guillermo Vazquez

Circulation Research 2010, 106:1479-1488: originally published online April 1, 2010
doi: 10.1161/CIRCRESAHA.109.213314
Circulation Research is published by the American Heart Association. 7272 Greenville Avenue, Dallas, TX 72514
 Print ISSN: 0009-7330. Online ISSN: 1524-4571

The Constitutive Function of Native TRPC3 Channels Modulates Vascular Cell Adhesion Molecule-1 Expression in Coronary Endothelial Cells Through Nuclear Factor κB Signaling

Kathryn Smedlund, Jean-Yves Tano, Guillermo Vazquez

Rationale: Upregulation of endothelial vascular cell adhesion molecule (VCAM)-1 and the subsequent increase in monocyte recruitment constitute critical events in atherogenesis. We have recently shown that in human coronary artery endothelial cells (HCAECs) regulated expression of VCAM-1 depends, to a significant extent, on expression and function of the Ca^{2+}-permeable channel transient receptor potential canonical (TRPC)3, regardless of the ability of the stimulatory signal to induce regulated Ca^{2+} influx, leading to the hypothesis that TRPC3 constitutive, rather than regulated function, contributes to the underlying signaling mechanism.

Objective: The present studies addressed this important question and gathered mechanistic insight on the signaling coupling constitutive TRPC3 function to VCAM-1 expression.

Methods and Results: In HCAECs, maneuvers that prevent Ca^{2+} influx or knockdown of TRPC3 markedly reduced tumor necrosis factor (TNF)α-induced VCAM-1 and monocyte adhesion. TNFα also induced TRPC3 expression and TRPC3-mediated constitutive cation influx and currents. Stable (HEK293 cells) or transient (HCAECs) overexpression of TRPC3 enhanced TNFα-induced VCAM-1 compared to wild-type cells. IκBα phosphorylation/degradation was reduced by TRPC3 knockdown and increased by channel overexpression. Inhibition of calmodulin completely prevented nuclear factor κB activation, whereas blocking calmodulin-dependent kinases or NADPH oxidases rendered partial inhibition.

Conclusions: Our findings indicate that in HCAECs expression of VCAM-1 and monocyte adhesion depend, to a significant extent, on TRPC3 constitutive function through a signaling mechanism that requires constitutive TRPC3-mediated Ca^{2+} influx for proper activation of nuclear factor κB, presumably through Ca^{2+}-dependent activation of the calmodulin/calmodulin-dependent kinase axis. (*Circ Res*. 2010;106:1479-1488.)

Key Words: TRPC3 ■ VCAM-1 ■ constitutive Ca^{2+} influx ■ NFκB signaling ■ atherogenesis

Atherosclerosis is a chronic inflammatory disease of the vascular wall that constitutes a major cause of cardiovascular morbidity/mortality in western societies.[1] Over the last 2 decades, basic and clinical research underscored the critical role of vascular inflammation not only in initiation but also in progression of the disease and extent of its complications. Recruitment of circulating monocytes to the endothelium and their migration into the subintima is a fundamental event in early and advanced stages of atherosclerosis.[2,3] Monocyte adhesion to endothelium requires interaction of the integrin $\alpha_4\beta_1$ on the monocyte with vascular cell adhesion molecule (VCAM)-1 on the endothelial cell.[4] Expression of VCAM-1 is upregulated in response to proinflammatory/proatherogenic stimuli, such as nucleotides, interleukin-1β, and oxidized low density lipoproteins, among others.[5] In human coronary artery endothelial cells (HCAECs) nucleotides activate $P2Y_2$ receptors to induce VCAM-1 through a mechanism that in part requires Ca^{2+} signaling.[6–10] Recently,[11] we showed that in HCAECs native TRPC3, a member of the transient receptor potential canonical (TRPC) family of nonselective cation channels,[12] contributes to the Ca^{2+} influx that follows stimulation of $P2Y_2$ receptors, and that TRPC3 expression is fundamental in the signaling underlying ATP-induced VCAM-1 and monocyte adhesion. Treatment with ATP also promotes augmented TRPC3 expression, and an increase in constitutive cation influx is detectable even after the acute phase of channel stimulation has subsided.[11] Tumor necrosis factor (TNF)α also induces VCAM-1 in endothelium from most vascular beds[13] including HCAECs.[11] Despite the fact that TNFα signaling is not associated to regulation of Ca^{2+} influx,[14] omission of extracellular Ca^{2+} impairs the ability of TNFα to induce VCAM-1 in HCAECs.[11] These observations, together with the fact that in native and heterologous expression systems TRPC3 forms channels endowed

Original received August 8, 2009; resubmission received November 16, 2009; revised resubmission received March 9, 2010; accepted March 18, 2010.

From the Department of Physiology and Pharmacology (K.S., J.-Y.T., G.V.) and Center for Diabetes and Endocrine Research (G.V.), University of Toledo College of Medicine, Ohio.

Correspondence to Guillermo Vazquez, Department of Physiology and Pharmacology, Mail Stop 1008, University of Toledo College of Medicine, Health Science Campus, 3000 Arlington Ave, Toledo, OH 43614. E-mail Guillermo.Vazquez@utoledo.edu

Circulation Research **is available at http://circres.ahajournals.org** **DOI: 10.1161/CIRCRESAHA.109.213314**

Non-standard Abbreviations and Acronyms

ApoE	apolipoprotein E
CAM	calmodulin
CAMK	calmodulin-dependent kinase
HA	hemagglutinin
HCAEC	human coronary artery endothelial cell
HPAEC	human pulmonary artery endothelial cell
HUVEC	human umbilical vein endothelial cell
ICAM	intercellular adhesion molecule
IKK	IκB kinase
IL	interleukin
NFκB	nuclear factor κB
OAG	1-oleyl-2-acetyl-*sn*-glycerol
siRNA	small interfering RNA
TNF	tumor necrosis factor
TRPC	transient receptor potential canonical
VCAM	vascular cell adhesion molecule

with high constitutive, nonregulated activity,[12,15] led us to hypothesize that TRPC3 constitutive, rather than regulated, function contributes to the mechanism driving VCAM-1 expression and monocyte adhesion in these cells. In the present work, we show that those 2 events depend, to a significant extent, on upregulated expression of native TRPC3 and the consequent gain in constitutive channel function. Mechanistic insight is provided suggesting a role for the calmodulin (CAM)/calmodulin-dependent kinase (CAMK)II axis in coupling constitutive TRPC3 function to activation of NFκB. We discuss our findings within the context of the potential impact of upregulated expression of a channel endowed with high constitutive activity in atherogenesis.

Methods

Cell culture and transfections, immunoblotting, cell ELISA, monocyte adhesion, Ca^{2+} imaging, and electrophysiological measurements were performed essentially as described previously.[11,16,17] Protocols, composition of solutions and buffers, sequence of small interfering (si)RNA oligonucleotides, and source of antibodies are provided in the Online Data Supplement, available at http://circres.ahajournals.org.

Results

Treatment of HCAECs with TNFα (10 ng/mL) resulted in robust expression of VCAM-1 already after 3 hours of treatment, remaining elevated for up to 16 hours (Online Figure I; also elsewhere[11,18]). TNFα effect was manifest in total (whole lysate, Figure 1A, $+Ca^{2+}$ lanes) and plasma membrane (Figure 1B) VCAM-1, with increased adhesion of U937 monocytes to HCAECs (Figure 1C). When studying the role of regulated Ca^{2+} influx on ATP-induced VCAM-1,[11] we found that omission of Ca^{2+} in the extracellular bath (nominally Ca^{2+}-free medium) also impaired the ability of TNFα to induce plasma membrane VCAM-1. The experiments in Figure 1 show that not only surface VCAM-1 (Figure 1B and elsewhere[11]) but also total VCAM-1 protein (Figure 1A, $-Ca^{2+}$ lanes; normalized densitometric values in the absence of Ca^{2+}: 0.081±0.010 0.096±0.015 VCAM-1/GAPDH, for control versus TNFα-treated cells, respectively, not statistically different, n=3) and monocyte adhesion (Figure 1C) were reduced when Ca^{2+} was omitted in the bath. This was unexpected considering that TNFα, unlike ATP, is not associated to regulated Ca^{2+} influx in endothelium. In fact, acutely challenging HCAECs with TNFα did not result in noticeable Ca^{2+} release or influx (Figure 2A) or changes in whole-cell currents (inward currents at −60 mV: −1.10±0.14 versus −1.40±0.10 pA/pF, outward currents at +60 mV: 2.10±0.20 versus 1.90±0.11 pA/pF, for control versus TNFα-treated cells, respectively; n=6 to 8 cells/condition, $P<0.07$, not statistically significant; see also Online Figure II, A). Because TRPC3 is a nonselective cation channel that can permeate Na^+ under physiological conditions (see[12] and references therein), we tested the possibility that membrane depolarization subsequent to TRPC3-mediated Na^+ influx could be masking any potential effect of TNFα on Ca^{2+} entry in the Fura-2 measurements, as in those experiments membrane potential is not clamped and thus subject to changes depending on ion movements across the membrane. Cells were challenged with TNFα but in the presence of *N*-methyl-D-glucamine as a substitute for Na^+ in the bath -thus preventing or minimizing membrane depolarization-; still, no changes in Ca^{2+} influx were observed (not shown). Altogether, these findings strongly suggested that if Ca^{2+} influx contributed to TNFα-dependent expression of VCAM-1, it was likely through constitutive, nonregulated channel function. To more directly explore this, HCAECs were exposed to TNFα (10 ng/mL, 3 hour) but in the presence of the Ca^{2+} channel blockers Gd^{3+} or SKF96365. As shown in Figure 2B and 2C, those blockers, at concentrations that abolish Ca^{2+} influx in HCAECs[11] (regulated and constitutive Ca^{2+} influx were inhibited by 94±2% with 10 μmol/L Gd^{3+} or 30 μmol/L SKF96365; see Online Figure III, B) markedly reduced TNFα-induced VCAM-1 and monocyte adhesion.

Combining real-time fluorescence measurements of Ba^{2+} influx with a siRNA approach we demonstrated that in HCAECs constitutive cation (Ca^{2+}/Ba^{2+}) entry is mediated by native TRPC3 channels[11] (and Online Figure III, C). Using this strategy, we examined if TRPC3-mediated nonregulated cation influx contributed to TNFα actions in these cells. HCAECs were transfected with TRPC3 siRNA (see the Online Data Supplement and Online Figure IV) and 48 hours later surface VCAM-1 and monocyte adhesion were evaluated. Figure 2B and 2C shows that both events were reduced when TRPC3 was knocked down. (Expression of TNFα receptor type-1 [TNFR1], evaluated by immunoblot, did not change under the different experimental conditions [normalized densitometric mean±SEM value for TNFR1/GAPDH was 1.032±0.29, for conditions including omission of Ca^{2+} in the bath, channel blockers, or siRNA transfections].) importantly, knockdown of the close TRPC3 relatives TRPC6 and -7 had no effect (Figure 2B and 2C; also Online Figure V). Moreover, cotransfecting HCAECs with TRPC3 siRNA and a TRPC3 encoding plasmid, rescued the siRNA effect (normalized densitometric values for total VCAM-1: 0.433±0.070 versus 0.395±0.080 VCAM-1/GAPDH, for

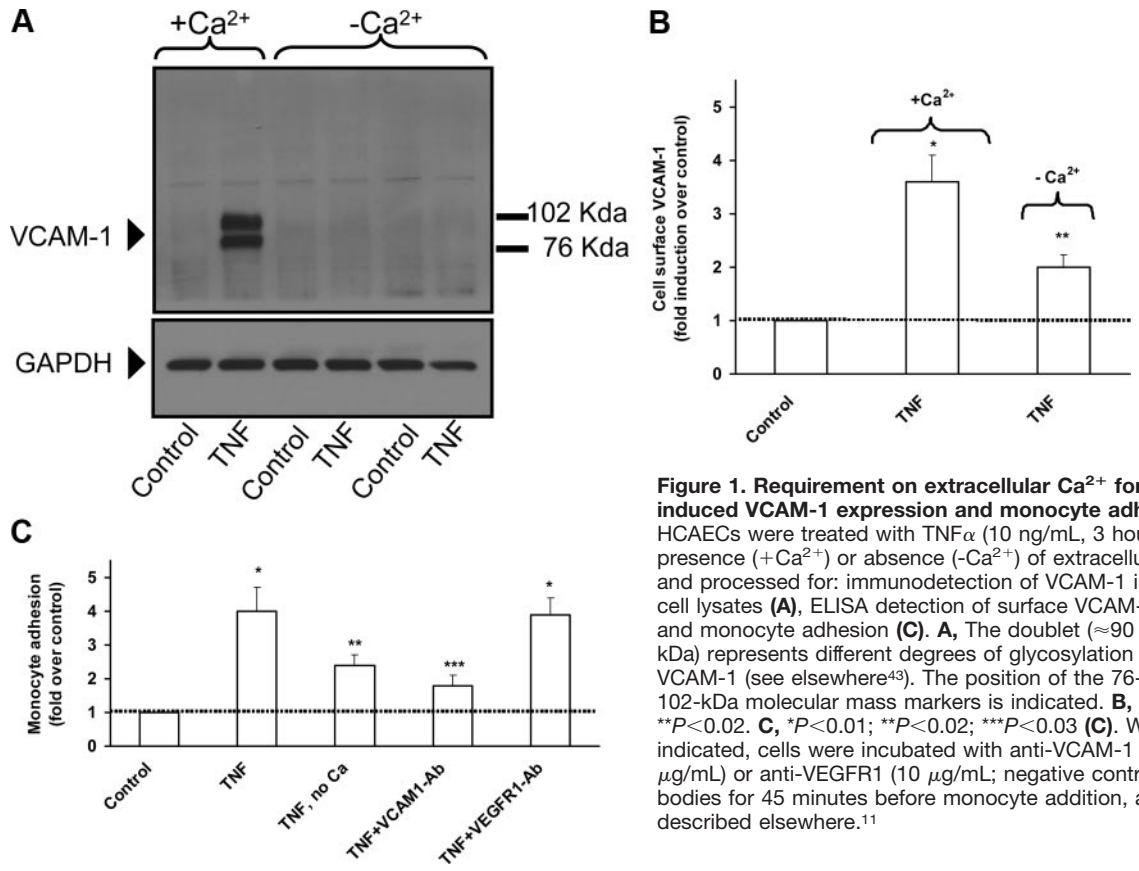

Figure 1. Requirement on extracellular Ca^{2+} for TNFα-induced VCAM-1 expression and monocyte adhesion. HCAECs were treated with TNFα (10 ng/mL, 3 hour) in the presence ($+Ca^{2+}$) or absence ($-Ca^{2+}$) of extracellular Ca^{2+} and processed for: immunodetection of VCAM-1 in whole cell lysates **(A)**, ELISA detection of surface VCAM-1 **(B)**, and monocyte adhesion **(C)**. **A,** The doublet (≈90 to 105 kDa) represents different degrees of glycosylation of VCAM-1 (see elsewhere[43]). The position of the 76- and 102-kDa molecular mass markers is indicated. **B,** $^{*}P<0.01$; $^{**}P<0.02$. **C,** $^{*}P<0.01$; $^{**}P<0.02$; $^{***}P<0.03$ **(C)**. When indicated, cells were incubated with anti-VCAM-1 (10 μg/mL) or anti-VEGFR1 (10 μg/mL; negative control) antibodies for 45 minutes before monocyte addition, as described elsewhere.[11]

control TNFα-treated versus "rescued" TNFα-treated cells, respectively; not statistically different, n=3; see also Online Figure VI). Intercellular adhesion molecule (ICAM)-1, but not E-selectin, was also upregulated after 3 hours of treatment of HCAECs with TNFα (Online Figure VII). Knockdown of TRPC3 drastically reduced TNFα-induced ICAM-1 total protein (Online Figure VII) but not surface ICAM-1 (not shown). To examine whether TRPC3 also contributed to the action of other proinflammatory/proatherogenic stimuli in HCAECs, we tested the effect of interleukin (IL)-1β and lipopolysaccharide on VCAM-1 expression. After 3 hours of treatment, IL-1β (10 ng/mL) but not lipopolysaccharide (from *Escherichia coli*, 1 μg/mL), induced VCAM-1 expression to a level comparable to that of TNFα (Online Figure VIII). TRPC3 knockdown reduced IL-1β effect by ≈41% (normalized densitometric values for IL-1β–induced VCAM-1: 0.352±0.040 versus 0.156±0.030, for cells transfected with nonspecific oligos versus TRPC3 siRNA, respectively; $P<0.05$, n=3).

Treatment with TNFα also resulted in a gain in basal cation entry (≈2-fold increase in rate of constitutive Ba^{2+} influx, Figure 3A and 3B), which correlated with a prominent increase in whole-cell current density (Figure 3C; Online Figure II, B) and amount of TRPC3 protein (Figure 3D). Remarkably, those effects were absent when TRPC3 was knocked down before TNFα treatment (Figure 3A through 3C). Constitutive Ba^{2+} influx remained unaffected by knockdown of TRPC6 or 7 (Online Figure III, C), supporting the notion that constitutive cation influx in HCAECs is mostly mediated by TRPC3.[11] TRPC4 and -7 proteins were also increased by TNFα, whereas TRPC1 was reduced to almost undetectable levels (Online Figure IX). TRPC5 and -6 remained unaltered (data not shown). To gather preliminary insight regarding expression of native TRPC3 in vivo, we examined TRPC3 by immunohistochemistry in aortic root sections from apolipoprotein (Apo)$E^{-/-}$ and wild-type (C57BL/6) mice (Online Figure X; see expanded Methods section in the Online Data Supplement). As expected, $ApoE^{-/-}$ mice showed unequivocal lesions which stained positive for neutral lipids and exhibited significant macrophage infiltration (Online Figure X, A through C). TRPC3 immunoreactivity in sections from wild-type animals, when present, was barely detectable or only manifested as few positive cells. TRPC3 staining, although diffuse, was more notorious in sections from $ApoE^{-/-}$ mice (Online Figure X, D through F).

Constitutive Ca^{2+} influx in HCAECs is masked by an efficient Ca^{2+} buffering system.[11] Despite that acute stimulation of these cells with TNFα did not induce any noticeable Ca^{2+} influx, the possibility remained that if TNFα were to promote weak activation of native TRPC3, the subsequent Ca^{2+} entry might be rapidly coped by the buffering apparatus thus going undetectable under our experimental conditions. However, even when Ba^{2+} was used as a surrogate for Ca^{2+} (Ba^{2+} is not substrate for buffering systems, enters cells unidirectionally and magnifies the otherwise unnoticeable basal cation influx; see[15]), acutely challenging HCAECs with TNFα did not result in detectable Ba^{2+} entry (rate of Ba^{2+}

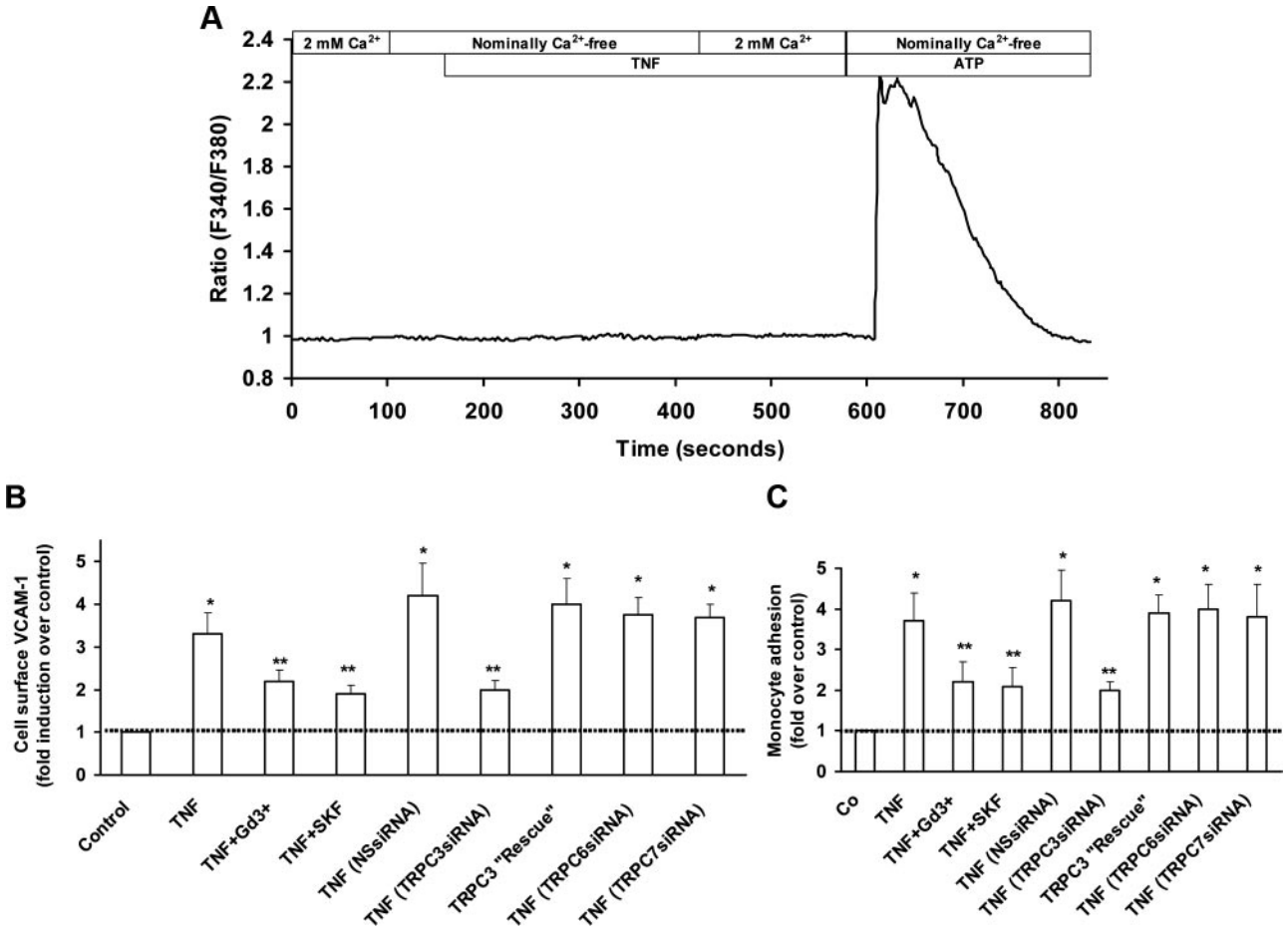

Figure 2. Requirement on native TRPC3 for TNFα-induced VCAM-1 expression and monocyte adhesion. A, Fura-2–loaded HCAECs were acutely exposed to TNFα (10 ng/mL) to evaluate changes in intracellular Ca^{2+}. Shown is the average response of 12 cells, representative of 51 cells from four independent experiments. Before ending the recording, cells were challenged with ATP (100 μmol/L) to test for responsiveness (see also[10,29]). **B,** HCAECs were treated with TNFα (10 ng/mL, 3 hour) in the presence or absence of the channel blockers Gd^{3+} (10 μmol/L) or SKF96365 (SKF) (30 μmol/L) and processed for detection of surface VCAM-1. Alternatively, cells were transfected with nonspecific oligonucleotides (NSsiRNA); siRNA specific for TRPC3 (TRPC3siRNA), TRPC6 (TRPC6siRNA), or TRPC7 (TRPC7siRNA); or cotransfected with TRPC3 siRNA plus TRPC3-HA cDNA (TRPC3 Rescue) (see expanded Methods in the Online Data Supplement) and, 48 hours later, treated with TNFα (10 ng/mL, 3 hour) and surface VCAM-1 detected by ELISA. *$P<0.01$; **$P<0.02$. **C,** HCAECs were treated as in **B** and then processed for evaluation of monocyte adhesion. *$P<0.01$; **$P<0.02$. Shown are results from 3 independent experiments.

influx: 0.015 ± 0.002 versus 0.011 ± 0.003 ratio units/min, for nontreated versus TNFα-treated cells, respectively; $P<0.08$, not statistically different; n=25 to 30 cells). To more directly assess whether TNFα had any effect on TRPC3, we used HEK293 cells stably overexpressing human TRPC3 (T3-HEK293[19]; Online Figure XI, B). As expected, T3-HEK293 cells responded to the diacylglycerol analog 1-oleyl-2-acetyl-*sn*-glycerol (OAG) (a potent TRPC3 activator in overexpression systems[15]) with robust regulated Ba^{2+} influx, a manifestation of overexpressed TRPC3[16,20] (data not shown); nevertheless, acute treatment with TNFα did not affect basal cation influx (rate of constitutive Ba^{2+} influx: 0.030 ± 0.002 versus 0.027 ± 0.001 ratio units/min, for nontreated versus acutely TNFα-treated cells, respectively; $P<0.07$, not statistically different, n=45 to 60 cells). We next asked whether the increase in TRPC3 expression, and thus in constitutive Ca^{2+} influx, is sufficient to promote VCAM-1 expression. To address this, 2 alternative approaches were undertaken. First, we examined VCAM-1 expression in T3-HEK293 cells. Because of the high levels of TRPC3, T3-HEK293 cells exhibit robust constitutive cation entry compared to wild-type cells (rate of Ba^{2+} influx: 0.030 ± 0.002 versus 0.013 ± 0.002 ratio units/min, for T3-HEK293 versus wild-type HEK293 cells, respectively; $P<0.001$, n=45 to 55 cells; see also elsewhere[16,20]). As shown in Figure 4A, VCAM-1 expression in wild-type HEK293 cells was significantly augmented ($\approx$1.5-fold over basal, $P<0.05$) after 16 hour of treatment with TNFα (10 ng/mL). Notably, whereas basal VCAM-1 was not significantly different from wild-type cells, the time course for TNFα-induced VCAM-1 in T3-HEK293 cells was left-shifted, with a trend to be significantly augmented already at 3 hour (1.5-fold over basal) and a marked increase compared with wild-type cells at 16 hour ($\approx$2.2-fold over corresponding basal, $P<0.05$). Notably, in wild-type and T3-HEK293 cells, TNFα-induced VCAM-1 was decreased in the presence of 10 μmol/L Gd^{3+} (Figure 4A). Second, we examined basal and TNFα-induced VCAM-1 in HCAECs transiently overexpressing TRPC3. Cells were transfected

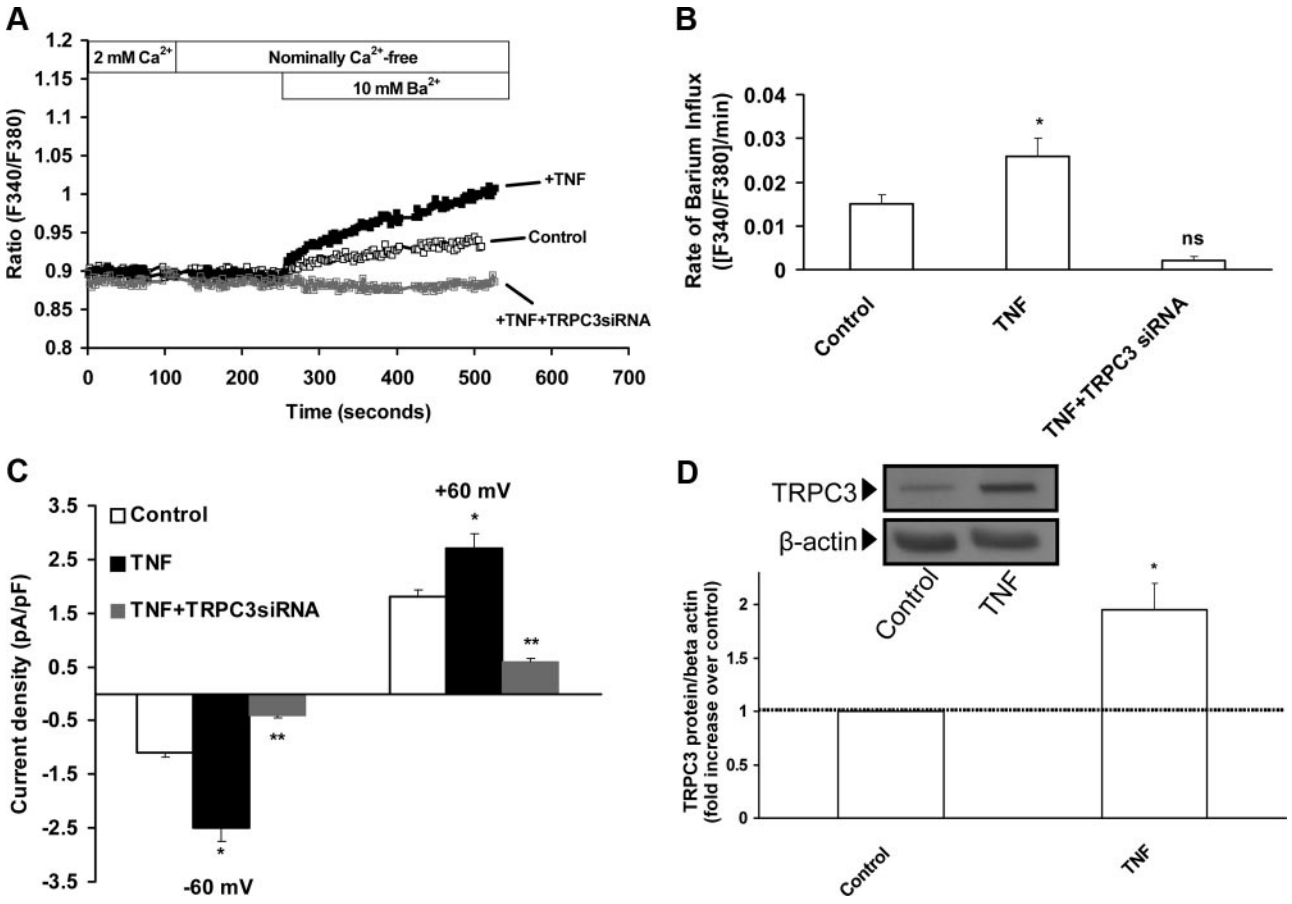

Figure 3. TNFα induces increased expression of constitutively active TRPC3 channels. A, HCAECs were transfected with TRPC3 siRNA **(gray square trace)** or nonspecific oligonucleotides **(empty and filled square traces)** and 48 hours later treated with TNFα (10 ng/mL, 3 hours; +TNF and TNF+TRPC3siRNA traces) or vehicle (control trace). After Fura-2 loading, the rate of constitutive Ba^{2+} (10 mmol/L) influx was determined by calculating the slope of fluorescence ratio increase (F340/F380 per minute) assessed within 2 minutes following Ba^{2+} addition. **B,** Averaged data (n=5) of rate of Ba^{2+} influx for conditions described in **A**. Absolute values for rate of fluorescence ratio are shown. *$P<0.01$; ns indicates not significantly different from fluctuations in basal fluorescence (ie, before Ba^{2+} addition). **C,** Transfections and treatment conditions of HCAECs were as in **A**. Whole-cell currents were measured as described in the expanded Methods section (see the Online Data Supplement) and normalized by cell capacitance (pA/pF). Shown are means±SEM of current densities at +60 and −60 mV for at least 8 cells per condition. *$P<0.01$ vs control; **$P<0.01$ vs the TNF condition, $P<0.01$ vs control, and not significantly different from leak currents. **D,** HCAECs were treated with TNFα (10 ng/mL, 3 hour) and processed for immunodetection of TRPC3. **Inset,** Representative blot. **Bar graph,** Average results of TNFα-induced TRPC3 protein derived from densitometric analysis; *$P<0.01$, n=5.

with a hemagglutinin epitope (HA)-tagged version of human TRPC3 (T3-HA, 1 μg; see also Online Figure XI, C). In mammalian cells, T3-HA trafficking, function, and regulation are indistinguishable from the nontagged channel.[16,20] T3-HA–transfected HCAECs, but not mock-transfected cells, exhibited a robust increase in constitutive and OAG-induced Ba^{2+} influx (rate of constitutive Ba^{2+} influx: 0.026±0.02 versus 0.012±0.002 ratio units/sec; rate of OAG-induced Ba^{2+} influx: 0.052±0.002 versus 0.015±0.003 ratio units/sec, for T3-HA-transfected versus mock-transfected cells, respectively; $P<0.01$, n=30 to 45 cells per group). (Despite expressing TRPC3/6/7 proteins,[11] HCAECs do not exhibit OAG-induced Ca^{2+} influx, likely because native TRPC3/6/7 proteins are inhibited by protein kinase [PK]C[22–24,] which is massively activated by the diacylglycerol analog. We have shown that native TRPC7 in lymphocytes[17,25] and native TRPC3 in HCAECs[26] respond to OAG only after PKC inhibition. Thus, under the present conditions [no PKC inhibition], OAG-induced Ba^{2+} influx is considered a manifestation of overexpressed TRPC3.) Whereas no differences were observed in basal VCAM-1 expression, TNFα-induced VCAM-1 was significantly higher in T3-HA-transfected HCAECs compared to mock transfected cells (Figure 4B).

In most endothelial cells, regulated expression of VCAM-1 (and ICAM-1) is driven by nuclear factor (NF)κB.[26] NFκB activation involves its release from the inhibitory IκBα protein, which requires phosphorylation of IκBα by IκB kinase (IKK)β followed by IκBα degradation.[27] Treatment of HCAECs with TNFα (10 ng/mL) resulted in rapid (peaking within 5 minutes) and sustained NFκB activation, as indicated by the extent of IκBα phosphorylation/degradation (Online Figure XII); both events were suppressed by the IKK inhibitor hypoestoxide (50 μmol/L, not shown), which also abolished TNFα-induced VCAM-1 (normalized densitometric values: 0.420±0.060 versus 0.050±0.010 VCAM-1/GAPDH, in the absence or presence of 50 μmol/L hypoestoxide, respectively). Because our data suggested a contribution of TRPC3 constitutive function to the mecha-

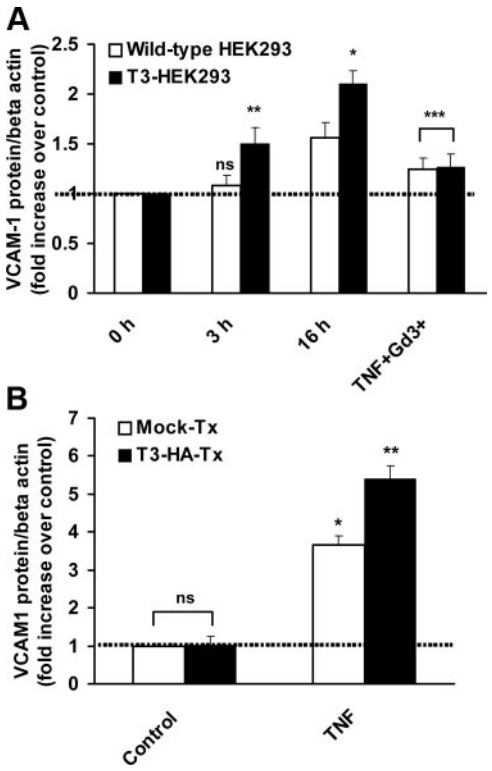

Figure 4. Overexpression of TRPC3 enhances TNFα-induced VCAM-1 expression. A, Wild-type HEK293 cells or T3-HEK293 cells were treated with TNFα (10 ng/mL) for the indicated times (or 16 hours when in the presence of 10 μmol/L Gd^{3+} [TNF+Gd3+]) and processed for immunodetection of total VCAM-1. Shown are average densitometric values of TNFα-induced VCAM-1. *$P<0.01$ vs control and $P<0.05$ vs the matching time point in wild-type HEK293 cells. **$P<0.05$ vs control and $P<0.06$ (not quite statistically different) vs matching time point in wild-type HEK293 cells; ***$P<0.05$ vs control and to matching time point in the absence of Gd^{3+}; ns: not significantly different from control. **B,** HCAECs were transfected with human TRPC3-HA (T3-HA-Tx) (see text for details) or vector alone (pcDNA3.1) (Mock-Tx). Forty-eight hours later, cells were treated with TNFα (10 ng/mL, 3 hour) and processed for immunodetection of total VCAM-1. *$P<0.01$ vs control; **$P<0.01$ vs control and $P<0.05$ vs TNFα-treated mock-transfected cells; ns: not significantly different from control. Shown are results from 3 independent experiments.

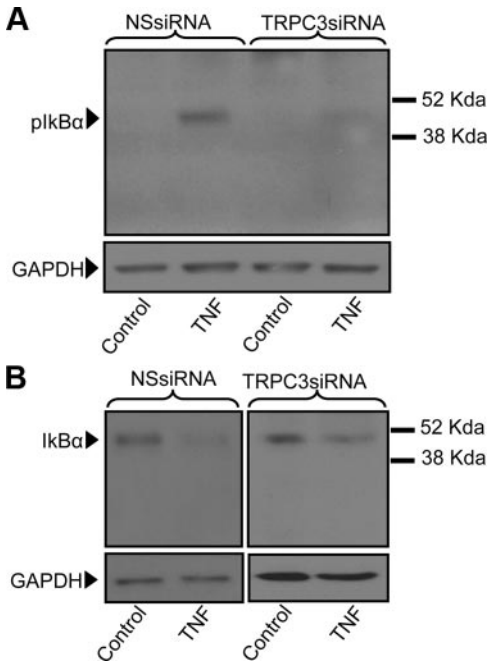

Figure 5. Knockdown of native TRPC3 reduces TNFα-induced activation of NFκB. HCAECs were transfected with nonspecific oligonucleotides (NSsiRNA) or siRNA specific for TRPC3 (TRPC3siRNA) and 48 hours later treated with TNFα (10 ng/mL, 5 minutes) and processed for immunodetection of phosphorylated IκBα (pIκBα) **(A)** and total IκBα **(B)**. Membranes were reprobed for GAPDH to control for protein loading. Blots are representative from 3 independent experiments. Position of the 38- and 52-kDa molecular mass markers is indicated.

nism driving VCAM-1 expression and considering that NFκB activation depends, directly or indirectly, on Ca^{2+} influx,[28] we speculated that TRPC3 might be required for activation of NFκB in HCAECs. As shown in Figure 5, knockdown of TRPC3 markedly decreased TNFα-induced IκBα phosphorylation (1.8- versus 5.1-fold increase over control, for TRPC3siRNA- versus NSsiRNA-transfected cells, respectively; n=3, $P<0.05$) and degradation (1.6- versus 2.8-fold reduction of control, for TRPC3siRNA- versus NSsiRNA-transfected cells, respectively; n=3, $P<0.05$). Conversely, transient overexpression of TRPC3-HA in HCAECs enhanced TNFα-induced IκBα phosphorylation (+1.3-fold) and degradation (+1.4-fold) compared with mock-transfected cells (n=3, $P<0.05$; Figure 6). Based on studies indicating that in several cell types, including endothelium (see elsewhere[29]), Ca^{2+} influx–dependent activation of NFκB is often associated to CAM and CAMKs, particularly CAMKII and CAMKIV, we undertook a pharmacological approach to gather preliminary insight on their potential participation in mediating the role of constitutive Ca^{2+} influx in activation of NFκB by TNFα in HCAECs. We focused on 2 of the earliest events associated to TNFα-dependent activation of the canonical NFκB route: phosphorylation of IκBα and its upstream regulator, IKKβ. As shown in Figure 7A, TNFα-induced phosphorylation of IKKβ was suppressed by the CAM inhibitor W-7 (50 μmol/L), the general CAMK antagonist KN-62 (10 μmol/L) and SKF96365 (which prevents constitutive Ca^{2+} influx in HCAECs; Online Figure III, B; and elsewhere[11]). Importantly, knockdown of TRPC3 also prevented TNFα-induced IKKβ phosphorylation. Similarly to IKKβ, phosphorylation of IκBα was completely abrogated by W-7 and SKF96365, and partially reduced by KN-62 (Figure 7B). Inhibition of NADPH oxidases with apocynin (0.5 mmol/L) resulted in partial decrease of IκBα phosphorylation (Figure 7B). (In HCAECs, membrane-associated, apocynin-sensitive NADPH oxidases [Nox2/Nox4A] are the major sources of TNFα-induced ROS.[30]) Neither basal nor TNFα stimulated phosphorylation of IκBα were affected by Gö6976 (1 μmol/L), a selective inhibitor of Ca^{2+}-dependent PKCs, or the phorbol ester PMA (0.1 mmol/L) (Online Figure XIII).

Discussion

The findings in the present work show that in HCAECs, TNFα-induced VCAM-1 and monocyte adhesion depend, to a considerable extent, on nonregulated Ca^{2+} influx through a

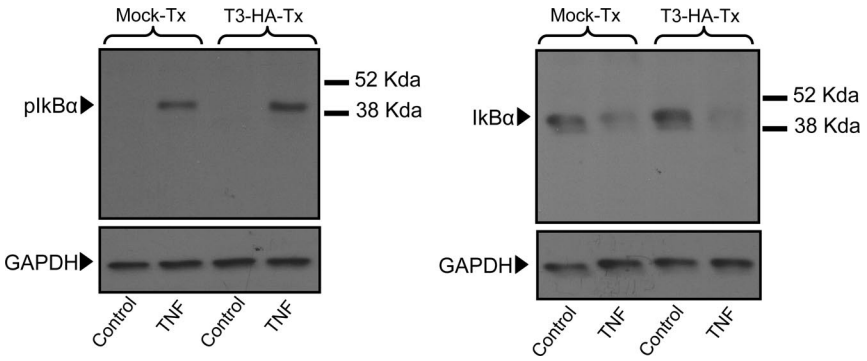

Figure 6. Overexpression of TRPC3 enhances TNFα-induced activation of NFκB. HCAECs transiently transfected with human TRPC3-HA (T3-HA-Tx) or vector alone (pcDNA3.1) (Mock-Tx) were treated with TNFα (10 ng/mL, 5 minutes) and processed for immunodetection of phosphorylated (pIκBα) and total IκBα (IκBα). Blots are representative from three independent experiments. Membranes were reprobed for GAPDH to control for protein loading. Position of the 38- and 52-kDa molecular mass markers is indicated.

mechanism that requires the constitutive function of TRPC3 channels. This is supported by several lines of evidence. First, maneuvers that prevent constitutive Ca^{2+} entry into cells or knockdown of native TRPC3 protein markedly impaired TNFα-induced VCAM-1 and monocyte adhesion. Second, regulated expression of VCAM-1 was enhanced in 2 different TRPC3-overexpression systems in the absence of receptor-dependent channel activation. Third, knockdown of TRPC3 drastically reduced activation of NFκB, which controls VCAM-1 expression in HCAECs.

Constitutive function of TRPC3 is inhibited by micromolar concentrations of the nonselective channel blockers SKF96365 and Gd^{3+}.[12] Whereas none of these compounds is specific for TRPC3, they reduced VCAM-1 expression and monocyte adhesion to the same extent as knockdown of TRPC3 did, supporting the notion that TRPC3 constitutive function contributes to those events. The partial reduction of surface VCAM-1 and monocyte adhesion when TRPC3 is knocked down can be attributed to incomplete downregulation of TRPC3 under our experimental conditions. However, constitutive Ca^{2+} influx, but not VCAM-1 or monocyte binding, was completely suppressed by Gd^{3+} and SKF96365, suggesting that in HCAECs, those processes are also regulated by alternative Ca^{2+}-independent mechanisms (see also elsewhere[11]). Importantly, our studies also show that in HCAECs TNFα-dependent activation of NFκB requires constitutive Ca^{2+} influx, presumably through TRPC3, which in HCAECs accounts for most of the constitutive Ca^{2+} entry (Figure 3B and 3C; Online Figure III, C; and elsewhere[11]). Indeed, TRPC3 knockdown significantly reduced TNFα-induced phosphorylation of IκBα and its upstream activator, IKKβ. Pharmacological inhibition of CAM or CAMKs drastically reduced TNFα-dependent phosphorylation of IKKβ and its target IκBα, pointing to the CAM/CAMK axis as a likely candidate in the mechanism coupling TRPC3-mediated constitutive Ca^{2+} influx to IKKβ phosphorylation and NFκB activation. Whereas KN-62 is equally efficient in inhibiting CAMKII or CAMKIV,[31] the predominant nuclear versus cytosolic localization of CAMKIV[31] suggests that is presumably CAMKII the one linking constitutive Ca^{2+} influx to NFκB. Interestingly, CAMKII is emerging as a critical CAMK in endothelial dysfunction within the context of cardiovascular disease.[32] The partial reduction of TNFα-induced IκBα phosphorylation by apocynin indicates that NADPH oxidase–mediated production of ROS is necessary for full activation of NFκB. (As indicated above, membrane-associated, apocynin-sensitive NADPH oxidases are the major sources of TNFα-induced ROS in HCAECs.[30]) However,

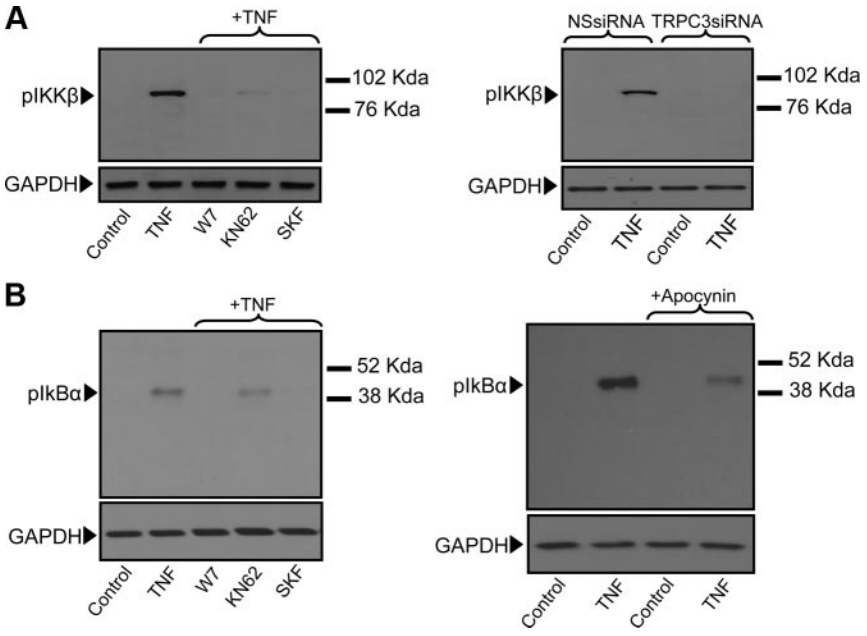

Figure 7. Role of Ca^{2+}, CAM/CAMK, ROS, and TRPC3 in TNFα-induced activation of NFκB. HCAECs were treated with TNFα (10 ng/mL, 5 minutes) in the absence or presence (15 minutes preincubation) of W-7 (50 μmol/L), KN-62 (10 μmol/L), SKF96365 (SKF) (30 μmol/L) or apocynin (0.5 mmol/L); alternatively, cells were transfected with nonspecific oligonucleotides (NSsiRNA) or TRPC3 siRNA (TRPC3siRNA), and 48 hours later treated with TNFα (10 ng/mL, 5 minutes). Cells were then processed for immunodetection of phosphorylated IKKβ (pIKKβ) **(A)** or phosphorylated IκBα (pIκBα) **(B)**. Membranes were reprobed for GAPDH to control for protein loading. Representative blots are shown (n=3). Relevant molecular mass markers are indicated.

ROS are not sufficient, because in the presence of W-7 (which blocks CAM activity without interfering with the constitutive Ca^{2+} entry that might be necessary for proper ROS generation), phosphorylation of IκBα was totally abrogated. SKF96365, similarly to W-7, also prevented TNFα-induced phosphorylation of IKKβ and IκBα, suggesting a mandatory requirement for constitutive Ca^{2+} entry-mediated activation of CAM at least early in the signaling (see below). A molecular approach will be required to unequivocally identify the CAMK isoform involved and the putative downstream targets that, acting in concert with ROS, lead to IKKβ phosphorylation and activation of NFκB. Recent work showed that CAM couples receptor-regulated activity of TRPC1 and TRPC4 to thrombin-induced NFκB stimulation in human and mouse endothelial cells,[29] whereas TNFα signaling was Ca^{2+}-independent. Our findings represent the first evidence for a role of the Ca^{2+}/CAM/CAMK axis in TNFα-dependent activation of NFκB in endothelial cells and the first suggesting a requirement for TRPC3 constitutive function in that process. Knockdown of TRPC3 also reduced TNFα-induced ICAM-1 (also driven by NFκB[26]) and IL-1β–induced VCAM-1, indicating that TRPC3 may exert a more general role in NFκB-dependent regulated expression of these adhesion molecules by different proatherogenic stimuli, rather than a specific function in TNFα-induced VCAM-1. Unlike VCAM-1, TRPC3 knockdown reduced total ICAM-1 protein levels but not those in the cell surface, indicating that ICAM-1 trafficking might be slower than that of VCAM-1, precluding for changes in surface ICAM-1 to be seen after only three hours of TNFα treatment.

The increase in TRPC3-mediated constitutive cation influx, whole-cell ionic currents and TRPC3 protein that follows TNFα treatment indicates that in HCAECs augmented expression of TRPC3 in response to proatherogenic factors translates into more functional channels in the membrane. Because basal cytosolic Ca^{2+} levels were not affected by the increase in constitutively active TRPC3 (96$\pm$7 nmol/L, with or without TNFα treatment), we speculate that any effect of TRPC3-mediated constitutive Ca^{2+} influx should occur within the immediate vicinity of the channel; such localized changes may suffice to modulate signaling components in close proximity to TRPC3 without manifesting into changes in bulk cytosolic Ca^{2+} (subject to rapid Ca^{2+} buffering). In line with this, it should be noted that experiments involving inhibition of CAM and CAMKs were performed under constitutive Ca^{2+} influx conditions (TNFα does not stimulate Ca^{2+} entry), suggesting that highly localized elevations in submembranous Ca^{2+} under basal conditions might be responsible for signaling to NFκB, as shown in other cell types.[33]

Other groups have also observed TNFα-dependent modulation of Ca^{2+} influx in relation to TRPC function. In airway smooth muscle cells, TNFα increased constitutive Ca^{2+} entry that was abrogated by knockdown of TRPC3.[34] In those studies, TNFα augmented TRPC3, whereas TRPC1, -4, -5, and -6 remained unaltered.[34] TNFα-induced TRPC1 expression was observed in human endothelial cells from dermal microvessels, umbilical vein (HUVECs), and pulmonary artery (HPAECs).[35,36] In HUVECs and HPAECs, that was accompanied by augmented receptor-regulated Ca^{2+} influx, but the impact of TNFα on constitutive influx was not examined. Our studies in HCAECs show a differential effect of TNFα on individual TRPC members. Whereas TRPC3, -4, and -7 proteins were increased by the cytokine, TRPC1 was drastically reduced, an observation that contrasts with the studies above.[35,36] Although differences in experimental conditions may account for such disparate results, it is likely that responsiveness of individual TRPCs to TNFα actions vary, not only in different cell types but also throughout the vascular tree.

Altogether, our findings suggest that a gain in constitutively active TRPC3 may result in pathological Ca^{2+}-dependent signaling, even in the absence of receptor stimulation. This prompted us to ask whether a mere increase in the number of TRPC3 channels would be sufficient to promote VCAM-1 expression. Our experiments using 2 different TRPC3 overexpression systems indicate that whereas under basal conditions high constitutive channel function did not induced VCAM-1, regulated expression was increased. In line with this, TRPC3 overexpression enhanced TNFα-induced IκBα phosphorylation/degradation without altering basal activity. The simplest interpretation is that TRPC3 constitutive function is necessary but not sufficient and that a priming signal, such as TNFα, might be needed. However, 2 aspects of the overexpression systems used here should be noted. First, HEK293 cells (nonendothelial) do not express VCAM-1 as robustly as HCAECs, and they always require priming with TNFα. Second, in transient TRPC3 overexpression in HCAECs a low plasmid concentration was used; because increasing DNA copy number through plasmid copy number leads to increases in TRPC3 protein,[37] the possibility remains that if higher expression levels were attained, a threshold would be reached at which constitutive TRPC3 function per se would be sufficient to alter basal VCAM-1 levels even in the absence of a priming signal. Are there in vivo examples of biological consequences of a gain in TRPC3 constitutive activity? Studies on TRPC6 knockout mice show that compensatory upregulated expression of TRPC3 resulted in elevated contractility of aorta and cerebral arteries.[38] In mouse skeletal myocytes TRPC3 is increased by neuromuscular activity and this correlates with enhanced constitutive NFAT activity.[39] Acting as Ca^{2+} entry gates is not the only way TRPCs can influence intracellular Ca^{2+}. Because they are nonselective cation channels TRPCs can alter membrane potential by mediating Na^{+} influx thus modulating the driving force for Ca^{2+} entry and/or affecting the activity of voltage-gated Ca^{2+} channels. Also, TRPC3 is involved in modulation of IP_3-mediated Ca^{2+} release from endoplasmic reticulum.[40] Although the latter has not been yet demonstrated to operate in endothelial cells, it may be of particular relevance in the action of stimuli endowed with Ca^{2+}-mobilizing properties in endothelium, such as ATP.

TRPC channels participate in myriad Ca^{2+}-dependent events that are part of the endothelial cell physiology and are emerging as critical players in signaling events associated to cardiovascular disease.[11,41,42] A review of existing literature shows that the role of TRPC3 constitutive activity in cardiovascular pathophysiology has been scarcely examined or, in

some instances, overlooked. The present findings underscore the potential impact of upregulated expression of constitutively active TRPC3 within the context of molecular/cellular events that are critical in the pathogenesis of coronary artery disease. Aortic root sections from atherosclerotic ApoE$^{-/-}$ mice showed more notorious immunoreactivity for TRPC3 than sections from wild-type animals. Although suggestive, a multitude of inflammatory mediators underlie lesion development in vivo, and thus a causal relationship between increased expression of native TRPC3 and atherogenesis cannot be established at this time. Generation of mouse models of atherosclerosis in which TRPC3 expression can be manipulated (ie, conditional transgenic or knockout animals for TRPC3) would be required to properly appreciate the contribution of TRPC3 to lesion development in vivo.

Sources of Funding

This work was supported by the American Heart Association (SDG0635250N to G.V.) and University of Toledo College of Medicine.

Disclosures

None.

References

1. Rosamond W, Flegal K, Furie K, Go A, Greenlund K, Haase N, Hailpern SM, Ho M, Howard V, Kissela B, Kittner S, Lloyd-Jones D, McDermott M, Meigs J, Moy C, Nichol G, O'Donnell C, Roger V, Sorlie P, Steinberger J, Thom T, Wilson M, Hong Y; American Heart Association Statistics Committee and Stroke Statistics Subcommittee. Heart disease and stroke statistics–2008 update: a report from the American Heart Association Statistics Committee and Stroke Statistics Subcommittee. *Circulation.* 2008;117:e25–e146.
2. Hansson GK. Inflammation, Atherosclerosis, and Coronary Artery Disease. *N Engl J Med*. 2005;352:1685–1695.
3. Virmani R, Burke AP, Farb A, Kolodgie FD. Pathology of the Vulnerable Plaque. *J Am Coll Cardiol*. 2006;47:C13–C18.
4. Galkina E, Ley K. Vascular Adhesion molecules in atherosclerosis. *Arterioscler Thromb Vasc Biol*. 2007;107:149179.
5. Erlinge D, Burnstock G. P2 receptors in cardiovascular regulation and disease. *Purinergic Signal.* 2008;4:1.
6. Seye CI, Yu N, Gonzalez FA, Erb L, Weisman GA. The $P2Y_2$ nucleotide receptor mediates vascular cell adhesion molecule-1 expression through interaction with VEGF receptor-2 (KDR/Flk-1). *J Biol Chem*. 2004;279:35679–35686.
7. Seye CI, Yu N, Jain R, Kong Q, Minor T, Newton J, Erb L, Gonzalez FA, Weisman GA. The P2Y2 nucleotide receptor mediates UTP-induced vascular cell adhesion molecule-1 expression in coronary artery endothelial cells. *J Biol Chem*. 2003;278:24960–24965.
8. Quinlan KL, Naik SM, Cannon G, Armstrong CA, Bunnett NW, Ansel JC, Caughman SW. Substance P activates coincident NFAT- and NFkB-dependent adhesion molecule gene expression in microvascular endothelial cells through intracellular calcium mobilization. *J Immunol*. 1999;163:5656–5665.
9. Chen NX, O'Neill KD, Niwa T, Moe SM. Signal transduction of βm-induced expression of VCAM-1 and COX-2 in synovial fibroblasts. *Kidney Int*. 2002;61:414–424.
10. Allen S, Khan S, Tam S-p, Koschinsky M, Taylor P, Yacoub M. Expression of adhesion molecules by Lp(a): a potential novel mechanism for its atherogenicity. *FASEB J*. 1998;12:1765–1776.
11. Smedlund K, Vazquez G. Involvement of native TRPC3 proteins in ATP-dependent expression of VCAM-1 and monocyte adherence in coronary artery endothelial cells. *Arterioscler Thromb Vasc Biol*. 2008;28:2049–2055.
12. Vazquez G, Wedel BJ, Aziz O, Trebak M, Putney JW Jr. The mammalian TRPC cation channels. *Biochim Biophys Acta*. 2004;1742:21–36.
13. Kleemann R, Zadelaar S, Kooistra T. Cytokines and atherosclerosis: a comprehensive review of studies in mice. *Cardiovasc Res*. 2008;79:360–376.
14. Bradley JR. TNF-mediated inflammatory disease. *J Pathol*. 2008;214:149–160.
15. Trebak M, Vazquez G, Bird GS, Putney JW Jr. The TRPC3/6/7 subfamily of cation channels. *Cell Calcium*. 2003;33:451–461.
16. Vazquez G, Wedel BJ, Kawasaki BT, Bird GS, Putney JW Jr. Obligatory role of Src kinase in the signaling mechanism for TRPC3 cation channels. *J Biol Chem*. 2004;279:40521–40528.
17. Lievremont JP, Numaga T, Vazquez G, Lemonnier L, Hara Y, Mori E, Trebak M, Moss SE, Bird GS, Mori Y, Putney JW Jr. The role of canonical transient receptor potential 7 in B-cell receptor-activated channels. *J Biol Chem*. 2005;280:35346–35351.
18. Csiszar A, Smith K, Labinskyy N, Orosz Z, Rivera A, Ungvari Z. Resveratrol attenuates TNFalpha-induced activation of coronary arterial endothelial cells: role of NFkB inhibition. *Am J Physiol Heart Circ Physiol*. 2006;291:H1694–H1699.
19. McKay RR, Szymeczek-Seay CL, Lievremont JP, Bird GS, Zitt C, Jungling E, Luckhoff A, Putney JW Jr. Cloning and expression of the human transient receptor potential 4 gene: localization and functional expression of human TRP4 and TRP3. *Biochem J*. 2000;351(Pt 3):735–746.
20. Trebak M, St. J. Bird G, McKay RR, Birnbaumer L, Putney JW Jr. Signaling mechanism for receptor-activated canonical transient receptor potential 3 (TRPC3) channels. *J Biol Chem*. 2003;278:16244–16252.
21. Trebak M, Hempel N, Wedel BJ, Smyth JT, Bird GS, Putney JW Jr. Negative regulation of TRPC3 channels by protein kinase c-mediated phosphorylation of serine 712. *Mol Pharmacol*. 2005;67:558–563.
22. Venkatachalam K, Zheng F, Gill DL. Regulation of canonical transient receptor potential (TRPC) channel function by diacylglycerol and PKC. *J Biol Chem*. 2003;278:29031–29040.
23. Okada T, Inoue R, Yamazaki K, Maeda A, Kurosaki T, Yamakuni T, Tanaka I, Shimizu S, Ikenaka K, Imoto K, Mori Y. Molecular and functional characterization of a novel mouse transient receptor potential protein homologue TRP7. Ca^{2+}-permeable cation channel that is constitutively activated and enhanced by stimulation of G-protein-coupled receptor. *J Biol Chem*. 1999;274:27359–27370.
24. Vazquez G, Bird GSJ, Mori Y, Putney JW Jr. Native TRPC7 channel activation by an inositol trisphosphate receptor-dependent mechanism. *J Biol Chem*. 2006;281:25250–25258.
25. Vazquez G, Putney JW. Role of canonical transient receptor potential channels (TRPC) in receptor-dependent regulation of vascular cell adhesion molecule-1 in human coronary artery endothelium. *Arterioscler Thromb Vasc Biol*. 2006;26:e93.
26. Kim I, Moon S-O, Hoon Kim S, Jin Kim H, Soon Koh Y, Young Koh G. Vascular endothelial growth factor expression of ICAM-1, VCAM-1 and E-selectin through NFkB activation in endothelial cells. *J Biol Chem*. 2001;276:7614–7620.
27. Tergaonkar V. NFkB pathway: a good signaling paradigm and therapeutic target. *Int J Biochem Cell Biol*. 2006;38:1647–1653.
28. Han B, Logsdon CD. CCK stimulates mob-1 expression and NFkB activation via protein kinase C and intracellular Ca^{2+}. *Am J Physiol Cell Physiol*. 2000;278:C344–C351.
29. Bair AM, Thippegowda PB, Freichel M, Cheng N, Ye RD, Vogel SM, Yu Y, Flockerzi V, Malik AB, Tiruppathi C. Ca^{2+} entry via TRPC channels is necessary for thrombin-induced NFkB activation in endothelial cells through AMP-activated protein kinase and protein kinase C-delta. *J Biol Chem*. 2009;284:563–574.
30. Yoshida LS, Tsunawaki S. Expression of NADPH oxidases and enhanced H_2O_2-generating activity in human coronary artery endothelial cells upon induction with tumor necrosis factor-α. *Int Pharmacol*. 2008;8:1377–1385.
31. Enslen H, Sun P, Brickey D, Soderling SH, Klamo E, Soderling TR. Characterization of Ca^{2+}/CAMKIV. Role in transcriptional regulation. *J Biol Chem*. 1994;269:15520–15527.
32. Cai H, Liu D, Garcia JGN. CaM kinase II-dependent pathophysiological signalling in endothelial cells. *Cardiovasc Res*. 2008;77:30–34.
33. Meffert MK, Chang JM, Wiltgen BJ, Fanselow MS, Baltimore D. NFkB functions in synaptic signaling and behavior. *Nature Neurosci*. 2003;6:1072–1078.
34. White TA, Xue A, Chini EN, Thompson M, Sieck GC, Wylam ME. Role of transient receptor potential C3 in TNFalpha-enhanced calcium influx in human airway myocytes. *Am J Respir Cell Mol Biol*. 2006;35:243–251.
35. Paria BC, Malik AB, Kwiatek AM, Rahman A, May MJ, Ghosh S, Tiruppathi C. Tumor necrosis factor-alpha induces NFkB-dependent TRPC1 expression in endothelial cells. *J Biol Chem*. 2003;278:37195–37203.

36. Paria BC, Vogel SM, Ahmmed GU, Alamgir S, Shroff J, Malik AB, Tiruppathi C. Tumor necrosis factor-alpha-induced TRPC1 expression amplifies store-operated Ca^{2+} influx and endothelial permeability. *Am J Physiol Lung Cell Mol Physiol*. 2004;287:L1303–L1313.
37. Vazquez G, Wedel BJ, Trebak M, St John Bird G, Putney JW Jr. Expression level of the canonical transient receptor potential 3 (TRPC3) channel determines its mechanism of activation. *J Biol Chem*. 2003;278:21649–21654.
38. Dietrich A, Mederos Y, Schnitzler M, Gollasch M, Gross V, Storch U, Dubrovska G, Obst M, Yildirim E, Salanova B, Kalwa H, Essin K, Pinkenburg O, Luft FC, Gudermann T, L B. Increased vascular smooth muscle contractility in $TRPC6^{-/-}$ mice. *Mol Cell Biol*. 2005;25:6980–6989.
39. Rosenberg P, Hawkins A, Stiber J, Shelton JM, Hutcheson K, Bassel-Duby R, Shin DM, Yan Z, Williams RS. TRPC3 channels confer cellular memory of recent neuromuscular activity. *Proc Natl Acad Sci U S A*. 2004;101:9387–9392.
40. Bandyopadhyay BC, Ong HL, Lockwich TP, Liu X, Paria BC, Singh BB, Ambudkar IS. TRPC3 controls agonist-stimulated intracellular Ca^{2+} release by mediating the interaction between inositol 1,4,5-trisphosphate receptor and RACK1. *J Biol Chem*. 2008;283:32821–32830.
41. Nilius B, Droogmans G, Wondergem R. Transient receptor potential channels in endothelium: solving the calcium entry puzzle? *Endothelium*. 2003;10:5–15.
42. Yao X, Garland CJ. Recent developments in vascular endothelial cell transient receptor potential channels. *Circ Res*. 2005;97:853–863.
43. Rice GE, Munro JM, Bevilacqua MP. Inducible cell adhesion molecule 110 (INCAM-110) is an endothelial receptor for lymphocytes. A CD11/CD18-independent adhesion mechanism. *J Exp Med*. 1990;171:1369–1374.

Novelty and Significance

What Is Known?

- Recruitment of monocytes to the subendothelial milieu is a key event in atherogenesis and is mostly mediated by vascular cell adhesion molecule (VCAM)-1.
- Transient receptor potential canonical (TRPC) channels are among the most important Ca^{2+} permeable cation channels in endothelium, where they participate in both physiological and pathophysiological processes.
- In recent work, we identified TRPC3, a member of the TRPC family, as an obligatory component of the mechanism underlying regulated expression of VCAM-1 in coronary endothelium, pointing for a potential role of this channel in atherogenesis.

What New Information Does This Article Contribute?

- The present work shows that, in coronary endothelium, proatherogenic stimuli induce expression of TRPC3 and that the increase in plasma membrane constitutively active TRPC3 channels mediates the Ca^{2+} influx that supports regulated expression of VCAM-1, intercellular adhesion molecule-1, and monocyte adhesion.
- Evidence is provided indicating that TRPC3-mediated constitutive Ca^{2+} influx is coupled to activation of nuclear factor (NF)κB through Ca^{2+}-dependent activation of the calmodulin/calmodulin-dependent kinase axis.

Expression of TRPC3 in coronary endothelium is upregulated by proatherogenic factors. Because TRPC3 exhibits high constitutive, nonregulated activity, it was important to determine whether the contribution of TRPC3 to VCAM-1 expression and monocyte adhesion was through regulated or nonregulated function and how such activity couples to intracellular signaling. We show that not only VCAM-1 but also intercellular adhesion molecule-1 expression has an obligatory requirement for TRPC3 constitutive function. This is a highly novel concept because the participation of TRPCs in vascular inflammation has been associated with receptor-dependent channel activation rather than constitutive activity, underscoring the potential pathophysiological relevance of increased endothelial expression of constitutively active TRPC channels. Mechanistic insight is provided indicating that TRPC3-mediated constitutive Ca^{2+} influx couples to activation of the canonical NFκB pathway through Ca^{2+}-dependent activation of calmodulin and calmodulin-dependent kinases. Identifying novel players in the signaling pathway that controls the expression of cell adhesion molecules is imperative to expand the spectrum of existing potential molecular targets that can be exploited to develop effective antiinflammatory therapies for atherosclerosis. The recognition of TRPC3 as a novel component in such processes represents a major contribution in that direction.

Supplementary information

Methods

Cells and transfections: HCAECs (Lonza, CA) and U937 human monocytic cells (ATCC, VA) were grown as described in[1]. Human embryonic kidney (HEK293) cells stably expressing human TRPC3 (kindly provided by Dr. J.W. Putney Jr., NIEHS, NC) were grown as in[2]. siRNA oligonucleotides for TRPC3, 6 or 7 (siGENOME SMART pool duplexes, Dharmacon), TRPC3-HA (into pcDNA3.1, kindly provided by Dr. Lutz Birnbaumer, NIEHS, NC) or pcDNA3.1 were delivered to cells with Lipofectamine2000 (Invitrogen, CA). For either TRPC3, 6 or 7 siRNA duplexes were used as a pool of four duplexes (target sequences below) at a total final concentration of 100 nM.

siRNA target sequences:

Scrambled (non-specific oligonucleotide)	5'-UAGCGACUAAACACAUCAA
TRPC3-1	5'-PGUAUUCCCUAGGUCCUUCCUU
TRPC3-2	5'-PCAUUCCAAGAACCCAGACCUU
TRPC3-3	5'-PAUUGCAUGGAGAGCUUCCGUU
TRPC3-4	5'-PUGAUAGCUAUGGUCUGCUCUU
TRPC6-1	5'-GCAUACAUGUUUAGUGAUC
TRPC6-2	5'-UGAACGGCCUCAUGAUUAU
TRPC6-3	5'-CAUCAUUCAUUGCGAGAUU
TRPC6-4	5'-UAAAGGUUAUGUUCGGAUU
TRPC7-1	5'-AAACAAAUCUUCAGAGUGA
TRPC7-2	5'-GAAAUGGGCAUGCUGAAUU
TRPC7-3	5'-GGAUCAAACUCGCCAUUAA
TRPC7-4	5'-CGGCUUAUCUGAAGUAAUC

Transfected cells were used for experiments 48 hours after transfection. We have previously shown that the siRNA protocol used here efficiently and selectively knocks down TRPC3 in HCAECs without altering expression of other TRPCs[1]. Knockdown of TRPC3, 6 and 7 at the protein level is documented in Figures IV and V. For rescue experiments, HCAECs were co-transfected with TRPC3 siRNA (100 nM) plus 1 μg of TRPC3-HA cDNA (into pcDNA3.1) and 48 hours later processed for immunodetection of VCAM-1, surface VCAM-1 or monocyte adhesion. The siGENOME SMART pool duplexes used here, target 3'-UTR (untranslated regions) sequences in TRPC3 mRNA; the cDNA encoding for TRPC3-HA contains only the ORF sequence for TRPC3-HA and thus it is not targeted by the siRNA oligos; therefore, concomitant expression of TRPC3-HA results in the observed "rescued" phenotype. Human recombinant tumor necrosis factor α (TNFα, Calbiochem, CA) was from *E. coli*, and contamination with bacterial LPS was <<0.1 ng/μg of TNFα. At the concentration of TNFα used in the present studies (10 ng/ml) LPS contamination is estimated to be <<1 pg/ml; even at concentrations of LPS as high as 1 μg/ml we did not observe significant effects of LPS on VCAM-1 expression in HCAECs (Figure VIII). Therefore, any potential effect from LPS contamination during TNFα treatments can be neglected. LPS (from *E. coli*) and interleukin-1β were from Calbiochem.

Immunoblotting: Cells were processed for SDS-PAGE (10% acrylamide) and immunoblotting as in[1]. Primary antibodies were: anti-VCAM-1 (clone E-10, Santa Cruz, CA); anti-ICAM-1 (clone 0.N.146, Santa Cruz, CA); anti-E selectin (clone 1.BB.613, Santa Cruz, CA); anti-TNFR1 (Calbiochem); anti-TRPC1, anti-TRPC3 and anti-TRPC4 (Alomone Labs, Israel); anti-TRPC7 (kindly provided by Dr. W. Schilling, Case Western University School of Medicine, OH); anti-IkBα, anti-phosphoIkBα, anti-phospho-IKKβ (Ser177/181) (Cell Signaling, MA); anti-GFP (clone B-2, Santa Cruz, CA); anti-HA (clone 3F10, Roche, Germany); anti-beta actin (Millipore, MA); anti-GAPDH (clone 0411, Santa Cruz, CA). After incubation with the appropriate HRP-labelled secondary antibody, immunoreactive bands were visualized by ECL (Amersham, PA) and

quantified by densitometry within the linear range of the film. All blots for a particular experimental condition were analyzed by densitometry and the values for the band of interest were normalized by the densitometric values obtained for beta-actin or GAPDH, as indicated; means ± SEM were obtained and corresponding fold change values respect to controls calculated.

Cell ELISA: The protocol for cell surface VCAM-1, ICAM-1 or E-selectin (cell ELISA) was essentially as previously described[1]. HCAECs were grown to confluence in 96-well plates, and after the indicated treatments cells were fixed in 0.5% glutaraldehyde, non-specific sites blocked with 0.5% bovine serum albumin, and then sequentially incubated (1 h, 37°C) with either VCAM-1 (R&D Systems, MN), ICAM-1 or E-selectin monoclonal antibodies and peroxidase-conjugated anti-mouse antibody (Amershan). Peroxidase reaction was performed with 3,3′,5,5′-Tetramethylbenzidine (Sigma) and stopped with 2 N HCl within the linear range of color development (10-15 min). Cell surface VCAM-1, ICAM-1 or E-selectin was estimated as optical density at 450 nm after background subtraction (O.D. in the absence of primary antibody).

Monocyte adhesion: This was essentially as in [1]. HCAECs were grown to confluence in 24-well plates. After indicated treatments calcein-loaded U937 cells were added (50,000/well) and incubation proceeded for 45 min at 37°C. Following washes with PBS, bound monocytes were counted (3 fields/well, triplicates/condition). In siRNA experiments, transfected HCAECs were plated onto 24-well plates for 48 hours and then processed as above.

Real-time Fluorescence: Coverslip-plated cells loaded with Fura-2 were used to monitor changes of intracellular Ca^{2+} or Ba^{2+} by real-time fluorescence with a CCD camera-based imaging system (Intracellular Imaging Inc., Cincinnati OH) as previously described[1, 2]. Measurements were at room temperature and treatments were in HEPES-buffered saline solution (HBSS, in mM: 140 NaCl, 4.7 KCl, 1 $MgCl_2$, 10 glucose, 10 HEPES pH 7.4, 2 $CaCl_2$). When indicated, Fura-2 measurements were performed in the presence of N-methyl-D-glucamine (NMDG, 140 mM) as a substitute for external Na^+ to prevent or minimize Na^+-influx dependent membrane depolarization. We did not observe significant differences in the effect of TNFα or ATP[1] when Ca^{2+}/Ba^{2+} measurements were performed at 37°C compared to room temperature; because cellular loading of Fura-2/AM was performed at room temperature -to minimize dye compartmentalization, see for instance [3]- we proceeded with the recordings at room temperature to avoid additional and unnecessary temperature changes immediately before the measurements. “Nominally Ca^{2+}-free medium” means HBSS with no Ca^{2+} added (free Ca^{2+} <<5 μM). In transfection experiments GFP was used as a marker and measurements were on GFP^+ cells. Basal cytosolic Ca^{2+} levels were 96 ± 7 nM throughout several independent calibrations; however, because tabulated K_d values for Fura-2/Ca^{2+} were used –we have not determined the actual K_d in HCAEC’s cytosolic environment - Ca^{2+} values are only estimative; therefore, and for simplicity, the ratio of Fura-2 fluorescence (510 nm emission) when excited at 340 and 380 nm (F340/F380) was used to calculate peaks or rates of changes in fluorescence, as in [2].

Electrophysiology: Ionic currents were recorded using the patch-clamp technique in its whole-cell configuration using an Axopatch-200B amplifier (Axon Instruments, USA) essentially as in [4]. The resistance of the pipettes (borosilicate glass capillaries, World Precision Instruments, FL) varied between 3-5 MΩ when filled with intracellular solution (composition below). The extracellular solution (osmolarity 310 mosmol/l) contained (in mM): NaCl, 145; KCl, 5; CsCl 10, HEPES, 10; MgCl2, 1; CaCl2, 2; pH, 7.3 (adjusted with NaOH). The intracellular (pipette) solution contained (in mM): 145 Cs^+ methanesulfonate; 10 BAPTA; 10 HEPES; 1 $MgCl_2$; 2 MgATP; 3.2 $CaCl_2$, pH 7.2; the free Ca^{2+} concentration of this solution was 100 nM, calculated with MaxChelator program Winmaxc v2.4 [5]). All measurements were performed at room temperature (22 °C). After establishing the whole cell configuration, membrane potential was clamped to 0 mV, and 250-ms voltage ramps (-80 to +80 mV) were applied every 2 s. When needed, acute addition of TNFα to the external solution was carried out using a multibarrel

puffing micropipette with common outflow positioned in close proximity to the cell under examination, and the cell was constantly superfused with bath solution to reduce potential artifacts related to switching from static to moving solution. Signals were low-pass filtered (1 kHz), digitized (20 kHz) and analyzed with Clampfit 9.2 software (Axon Instr., USA). In transfection experiments GFP was used as a marker and measurements were on GFP^+ cells. Upon establishment of the whole-cell configuration, capacitive currents were compensated and measurements started within 30 seconds. Cell capacitances ranged between 40-75 pF.

Mice, aortic root sectioning and immunohistochemistry: All animal studies meet NIH guidelines and corresponding protocols have been approved by University of Toledo IACUC. We maintain our own colonies of C57BL/6 and $ApoE^{-/-}$ mice (originally obtained from Jackson Labs, ME) at the Division of Laboratory and Animal Research of the University of Toledo Health Science Campus. Starting at 6 week-old, male and female ApoE-deficient mice ($ApoE^{-/-}$, on C57BL/6 background) were kept on Western type diet (D12079B, Research Diets) during 21 weeks. Under these conditions, as expected, $ApoE^{-/-}$ mice developed significant lesions along the aortic root segment (Figure X); lesion development in $ApoE^{-/-}$ mice has been thoroughly characterized [6-8]. C57BL/6 mice were kept on regular chow diet for 21-weeks and used as controls. At the end of the 21 weeks, we evaluated lesion size and TRPC3 expression in aortic root sections. Gender differences in lesion size are not consistent throughout studies and some published evidence suggests that female mice tend to develop larger lesions than males (discussed in [9]). Under our own experimental conditions we found no significant differences in lesion area between male and females from $ApoE^{-/-}$ on Western type diet (lesion area: 742,300 ± 89,076 and 668,600 ± 73,500 μm^2, for male and female $ApoE^{-/-}$, respectively, $P<0.538$; n=6/group).

At euthanasia mice were perfused through the left ventricle with heparinized-PBS followed by 4% paraformaldehyde. The heart was removed and cut in the plane between the lower tips of the right and left atria, allowing cross-sections of all three aortic valves to be in the same geometric plane; the aorta was cut at the point where it emerges from the ventricle. The upper portion of the heart was put into a tissue mold, embedded in O.C.T. and frozen in the Peltier stage of the cryostat (Thermo Scientific R. Allan HM550 Cryostat). Blocks were processed immediately or stored at -20°C until sectioning. 10 µm thick cross-sections were collected starting at the point where aorta emerges from the ventricle (beginning of ascending aorta, sections round in appearance: stage I) and moving towards the aortic sinus (insinuation of aortic valves: stage II; appearance of clearly identifiable aortic valves: stage III; aortic sinus: stage IV), covering a distance of ~650-700 µm. Sections were collected onto Fisher Superfrost Plus-coated slides following a scheme similar to that described by Daugherty and Whitman [10]. Each slide (at least 5 slides per animal) contained 12 sections at 40 µm interval throughout the entire aortic root. Additional sections were collected at the end to be used as controls in subsequent immunostaining procedures. Sections were air-dried and stored (-80°C) until processed. Slides were processed for Oil Red O (ORO) staining or immunohistochemistry as described below.

Oil Red O (ORO) staining: Sections were fixed with 10% formalin, stained with ORO and counterstained with hematoxylin. Images of each section on a slide were captured using a digital camera (Micropublisher 3.3 Megapixel Cooled CCD Color Digital Camera coupled to Zeiss Axiovert 40CL inverted microscope) and lesion area was measured with image analysis software (NIS Elements D) by manually outlining each lesion as defined by the lumen boundary and the internal elastic lamina ($ApoE^{-/-}$ mice) using ORO staining as a visual aid only. Lesion size for each mouse was obtained as the total lesion area (in square micrometers) in 12 sections from the same mouse (at 40 µm interval throughout the aortic root).

Immunohistochemistry: Sections were fixed in acetone (-20°C, 10 min) and processed for immunostaining for TRPC3 using rabbit anti-TRPC3 (Alomone) followed by incubation with polyclonal swine anti-rabbit biotinylated immunoglobulins $(F(ab')_2$ (Dako, Denmark); immunostaining for MOMA-2 was performed using clone MCA519G (Serotec) followed by

incubation with biotinylated rabbit anti-rat antibody (Dako). In both instances, treatment with secondary antibodies was followed by incubation with alkaline phosphatase-conjugated streptavidin (Dako). The blocking step included 1% BSA plus normal swine serum (for TRPC3 staining) or 1% BSA alone (for MOMA-2 staining). Counterstaining was performed with hematoxylin and mounting with Ultramount (Dako). Negative controls were performed by omitting primary antibody.

Statistical analysis: Mean rates of Ba^{2+} entry and means for normalized densitometric values were compared using a two-tailed *t* test for two means, using Graph Pad InStat version 3.00 for Windows 95 (Graph Pad Software, San Diego CA). Averaged results are from 3-5 independent experiments. $P<0.05$ was considered significant.

Figure Legends

Supplementary Figure I.

HCAECs were treated with TNFα (10 ng/ml) for the indicated times and processed for immunodetection of VCAM-1 in whole cell lysates as described in Methods. The doublet (~90-105 kDa) in the immunoblot represents different extents of glycosylation of VCAM-1 (see for instance[11, 12]). For reference, the position of the 76 Kda and 102 Kda molecular weight markers is indicated.

Supplementary Figure II.

A) Time course of spontaneous, constitutive whole-cell currents in HCAECs, before and after acute addition of TNFα (10 ng/ml) to the external bath. Shown are average inward (-60 mV) and outward (+60 mV) currents from 4 individual cells. X-axis tick mark labels are shown in low position respect to the axis to avoid overlap with the inward current trace. **B)** Current-voltage (I/V) relationship for spontaneous, constitutive whole-cell currents before (black trace) and after (light and dark gray traces) 3 hour pre-treatment with TNFα (10 ng/ml), as indicated. It should be noted that, contrary to experiments in "A", light and dark gray I/V curves correspond to cells that were continuously exposed to TNFα for 3 hours before measurement of whole-cell currents (*i.e.*, no acute stimulation). The "Control" I/V curve is indistinguishable from the I/V relationships in experiments like those in "A" (*i.e.*, spontaneous whole-cell currents with or without acute TNFα addition). Whole-cell currents were measured as described in Methods and normalized by cell capacitance (pA/pF). Data are representative of independent measurements performed on at least eight single cells.

Supplementary Figure III.

A) In HCAECs activation of $P2Y_2$ receptors by ATP promotes a biphasic Ca^{2+} response, that consists of a transient PLC-dependent IP_3-mediated release of Ca^{2+} from internal Ca^{2+} stores followed by Ca^{2+} influx across the plasma membrane [1]. The Fura-2 measurements shown in panel A illustrate how when cells are challenged with ATP in nominally Ca^{2+}-free medium (filled squares trace) a rapid and transient increase in cytosolic Ca^{2+} takes place (IP_3-induced Ca^{2+} release). In the experiments shown here, once this Ca^{2+} transient was over, Ba^{2+} (10 mM) was added to the bath to evidence operation of a cation (Ca^{2+} and Ba^{2+} permeable[1]) influx route. Alternatively, cells were maintained in nominally Ca^{2+}-free medium (without ATP stimulation) and when indicated Ba^{2+} (10 mM) was added to the bath to evidence the existence of constitutive, non-regulated cation influx (empty squares trace). Traces are averages of 15-22 cells and are representative of at least four independent experiments. Values for rates of Ba^{2+} influx for ATP-induced (regulated) and constitutive (non-regulated) cation entry are shown as means ± SEM of fluorescence ratio per minute. **B)** Summarized data of the effect of the channel blockers Gd^{3+} (Gd3+, 10 μM) and SKF96365 (SKF, 30 μM) on either ATP-induced (Receptor-activated influx) or constitutive influx, expressed as percent of the rate of Ba^{2+} influx in the absence of blockers ("Control"). Results are from three independent experiments, each

performed on at least 15 cells; *P<0.001. **C)** HCAECs were transfected with siRNA specific for TRPC3, 6 or 7 or non-specific oligonucleotides ("Control") and 48 hours later loaded with Fura-2 to evaluate constitutive Ba^{2+} influx as in "A". Results are from three independent experiments, each performed on at least 8-10 transfected cells; *P<0.001; ns: not significantly different from control.

Supplementary Figure IV.
HCAECs were transfected with TRPC3 siRNA or non-specific oligonucleotides (NSsiRNA) and 48 hours later treated with TNFα (10 ng/ml, 3 h). Lysates were obtained and cellular proteins were immunoblotted for detection of TRPC3 as described in Methods. The lower portion of the membranes was cut and processed for immunodetection of beta-actin (β-actin) to control for protein loading. Shown is a representative blot from five independent experiments. In this particular case, normalized densitometric values (TRPC3/β-actin) showed a 1.7-fold increase in TRPC3 protein respect to control, which falls within the range of 1.95 ± 0.25 fold-increase respect to control in cells treated with TNFα (Figure 3D). The immunoblots were performed on lysates from the same batch of cells that were used for "NSsiRNA" and "TRPC3siRNA" conditions in the experiments in Figures 2B, 2C and 3A. For reference, the position of the 76 Kda and 102 Kda molecular weight markers is indicated.

Supplementary Figure V.
HCAECs were transfected with siRNA specific for TRPC6 or 7, or non-specific oligonucleotides (NSsiRNA). 48 hours later lysates were obtained and cellular proteins were immunoblotted for detection of TRPC6 and 7 as described in Methods. The lower portion of the membranes was cut and processed for immunodetection of GAPDH to control for protein loading. Shown are representative blots from three independent experiments. The immunoblots were performed on lysates from the same batch of cells that were used for "TRPC6siRNA" and "TRPC7siRNA" conditions in the experiments in Figures 2B, 2C and IIC. For reference, the position of the 76 Kda and 102 Kda molecular weight markers is indicated.

Supplementary Figure VI.
HCAECs were transfected with TRPC3 siRNA, non-specific oligonucleotides (NSsiRNA) or co-transfected with TRPC3 siRNA plus TRPC3-HA cDNA ("Rescue"). Forty eight hours later cells were treated with TNFα (10 ng/ml, 3 h), lysed, and cellular proteins were immunoblotted for detection of VCAM-1 as described in Methods. The lower portion of the membranes was cut and processed for immunodetection of GAPDH to control for protein loading. TNFα-induced VCAM-1 in the "Rescue" condition seems more robust than in NSsiRNA-transfected cells, probably reflecting the enhancing effect of TRPC3 overexpression on TNFα action (see for instance Figure 4B). Shown are blots representative from three independent experiments. For reference, the position of the 76 Kda and 102 Kda molecular weight markers is indicated.

Supplementary Figure VII.
HCAECs were transfected with TRPC3 siRNA or non-specific oligonucleotides (NSsiRNA) and 48 hours later treated with TNFα (10 ng/ml, 3 h). Lysates were obtained and cellular proteins were immunoblotted for detection of ICAM-1 as described in Methods. The lower portion of the membranes was cut and processed for immunodetection of GAPDH to control for protein loading. Shown are blots representative from two independent experiments. For reference, the position of the 76 Kda and 102 Kda molecular weight markers is indicated.

Supplementary Figure VIII.
HCAECs were treated with TNFα (10 ng/ml), LPS (from *E. coli*, 1 μg/ml) or IL-1β (human recombinant, 10 ng/ml) during 3 hours and then processed for immunodetection of VCAM-1 in

whole cell lysates as described in Methods. The lower portion of the membrane was cut and processed for immunodetection of GAPDH to control for protein loading. Shown is a representative blot from two independent experiments. For reference, the position of the 76 Kda and 102 Kda molecular weight markers is indicated.

Supplementary Figure IX.
HCAECs were treated with TNFα (10 ng/ml, 3 h) and processed for immunodetection of all TRPC family members. Shown are representative blots for those TRPCs that exhibited significant change after treatment (see text for details). The lower portion of the membranes was cut and processed for immunodetection of beta-actin (β-actin) to control for protein loading. For reference, the position of the 76 Kda and 102 Kda molecular weight markers is indicated.

Supplementary Figure X.
Photomicrographs of aortic root sections from ApoE$^{-/-}$ mice showing intima thickening, presence of lipid deposits and macrophage infiltration. **A)** Oil Red O staining of neutral lipids; original magnification X5. **B, C)** Macrophages were stained with MOMA-2 antibody; macrophage accumulation can be seen under the endothelium, with some immunoreactive areas separated by regions of non-stained cells and matrix. Original magnification X20. **D-F)** Immunostaining for TRPC3 in aortic root sections from wild-type (D) and ApoE$^{-/-}$ mice (E, F). In wild-type animals TRPC3 staining, when present, was manifested as few positive cells (arrowheads) or was barely visible at low power. TRPC3 staining was more notorious in lesions of ApoE$^{-/-}$ mice, with a patchy (E) or diffuse (F) staining. No gender differences in TRPC3 immunostaining were found for either wild-type or ApoE$^{-/-}$ animals. Original magnification X20.

Supplementary Figure XI.
Wild-type HEK293 cells (WtHEK293, panel **A**) or T3-HEK293 cells (**B**) were treated with TNFα (10 ng/ml) for the indicated times and processed for immunodetection of TRPC3. T3-HEK293 cells stably express a GFP-tagged version of TRPC3 (T3-GFP), and therefore anti-GFP was used for detection of overexpressed T3-GFP. Endogenous TRPC3 in wild-type HEK293 cells was detected with anti-TRPC3 antibody (Alomone Labs, Israel). The lower portion of the membranes was cut and processed for immunodetection of GAPDH to control for protein loading. **C)** HCAECs transiently expressing human TRPC3-HA ("T3-HA-Tx", see text for details) or vector alone (pcDNA3.1, "Mock-Tx") were lysed, TRPC3-HA was immunoprecipitated with anti-HA monoclonal antibody (Roche, Germany) and the membranes immunoblotted with the same antibody. **Note:** there is clearly a TNFα-dependent upregulation of T3-GFP in T3-HEK293 cells, likely due to the known responsiveness of the CMV promoter –which drives expression of the T3-GFP construct- to this cytokine[13]. There seemed to be a trend for TNFα to induce a slight increase (~15% above basal when normalized densitometric values are compared; n=2) in endogenous TRPC3 in wt-HEK293 cells after 16 hours of treatment, which coincides with the time at which VCAM-1 expression is significantly upregulated following cytokine treatment (see Figure 4A).

Supplementary Figure XII.
HCAECs were treated with TNFα (10 ng/ml) for the indicated times and then processed for immunodetection of phosphorylated IκBα (pIκBα, panel A) and total IκBα (panel B). Representative blot from three independent experiments. Membranes were reprobed for immunodetection of GAPDH to control for protein loading. For reference, the position of the 38 Kda and 52 Kda molecular weight markers is indicated.

Supplementary Figure XIII.
A) HCAECs were treated during 5 min with TNFα (10 ng/ml), PMA (0.1 mM) or TNFα+PMA. **B)** HCAECs were treated during 5 min with TNFα (10 ng/ml) in the presence or absence of Gö6976 ("Go+TNF", 1 μM, 15 min pre-treatment). In all instances cells were processed for immunodetection of phosphorylated IκBα (pIκBα) and membranes reprobed for immunodetection of GAPDH to control for protein loading. Shown are representative blots from two independent experiments. The position of the 38 Kda and 52 Kda molecular weight markers is indicated. **Note:** in "B" the blot corresponding to "Go+TNF" was boxed to denote the fact that it was cut from a different region of the same membrane and pasted next to "Control" and "TNF" for comparison purposes; however, all experimental conditions shown in "B" were blotted on the same PVDF membrane and ECL-developed simultaneously on the same film.

References

1. Smedlund K, Vazquez G. Involvement of Native TRPC3 Proteins in ATP-Dependent Expression of VCAM-1 and Monocyte Adherence in Coronary Artery Endothelial Cells. *Arterioscler Thromb Vasc Biol.* 2008;28:2049-2055.
2. Vazquez G, Wedel BJ, Kawasaki BT, Bird GS, Putney JW, Jr. Obligatory role of Src kinase in the signaling mechanism for TRPC3 cation channels. *J Biol Chem.* 2004;279:40521-40528.
3. Baldi C VG, Boland R. Capacitative calcium influx in human epithelial breast cancer and non-tumorigenic cells occurs through Ca2+ entry pathways with different permeabilities to divalent cations. *J Cell Biochem.* 2003;88:1265-1272.
4. Lievremont JP, Numaga T, Vazquez G, Lemonnier L, Hara Y, Mori E, Trebak M, Moss SE, Bird GS, Mori Y, Putney JWJ. The role of canonical transient receptor potential 7 in B-cell receptor-activated channels. *J Biol Chem.* 2005;280:35346-35351.
5. Bers D, Patton C, Nuccitelli R. A practical guide to the preparation of calcium buffers. *Methods Cell Biol.* 1994;40:3-29.
6. Reddick RL, Zhang SH, Maeda N. Atherosclerosis in mice lacking apo E. Evaluation of lesional development and progression. *Arteriosclerosis and thrombosis : a journal of vascular biology / American Heart Association.* 1994;14:141.
7. Fazio S, Linton MF. Mouse Models of Hyperlipidemia and Atherosclerosis. *Front Biosc.* 2001;6:515-525.
8. Nakashima Y, Plump AS, Raines EW, Breslow JL, Ross R. ApoE-deficient mice develop lesions of all phases of atherosclerosis throughout the arterial tree. *Arterioscler Thromb* 1994;14:133-140.
9. Daugherty A, Rateri DL. Development of experimental designs for atherosclerosis studies in mice. *Methods.* 2005;36:129-138.
10. Daugherty A, Whitman SC. Quantification of atherosclerosis in mice. *Methods in molecular biology (Clifton, N.J.).* 2003;209:293.
11. Rice GE, Munro JM, Bevilacqua MP. Inducible cell adhesion molecule 110 (INCAM-110) is an endothelial receptor for lymphocytes. A CD11/CD18-independent adhesion mechanism. *J Exp Med.* 1990;171:1369-1374.
12. Carlos TM, Schwartz BR, Kovach NL, Yee E, Rosa M, Osborn L, Chi-Rosso G, Newman B, Lobb R, Rosso M. Vascular cell adhesion molecule-1 mediates lymphocyte adherence to cytokine-activated cultured human endothelial cells [published erratum appears in Blood. 1990 1;76:2420]. *Blood.* 1990;76:965-970.
13. Stein J, Volk H-D, Liebenthal C, Kruger DH, Prosch S. Tumour necrosis factor {alpha} stimulates the activity of the human cytomegalovirus major immediate early enhancer/promoter in immature monocytic cells. *J Gen Virol.* 1993;74:2333-2338.

Supplementary Figure I

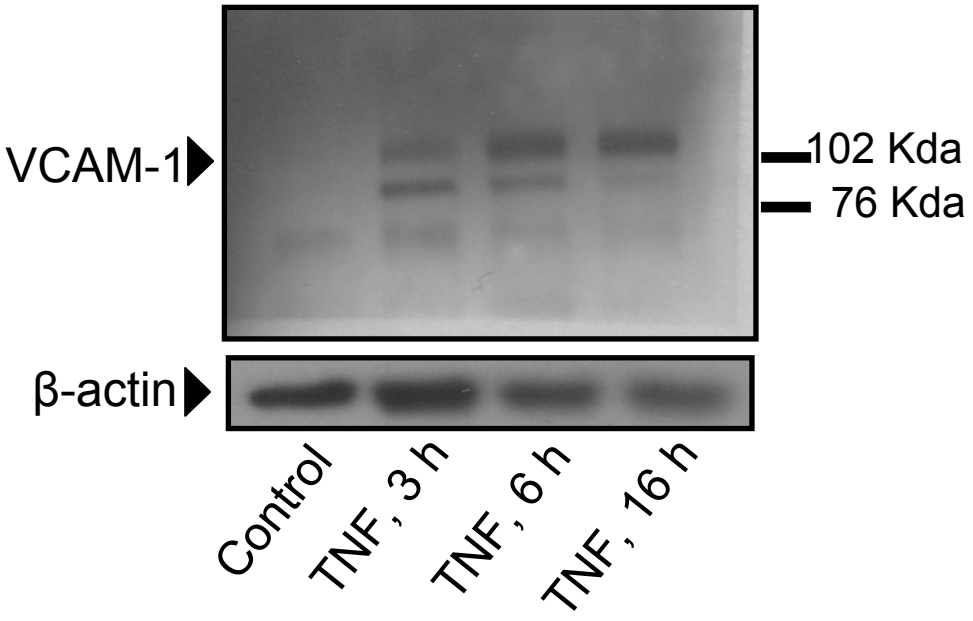

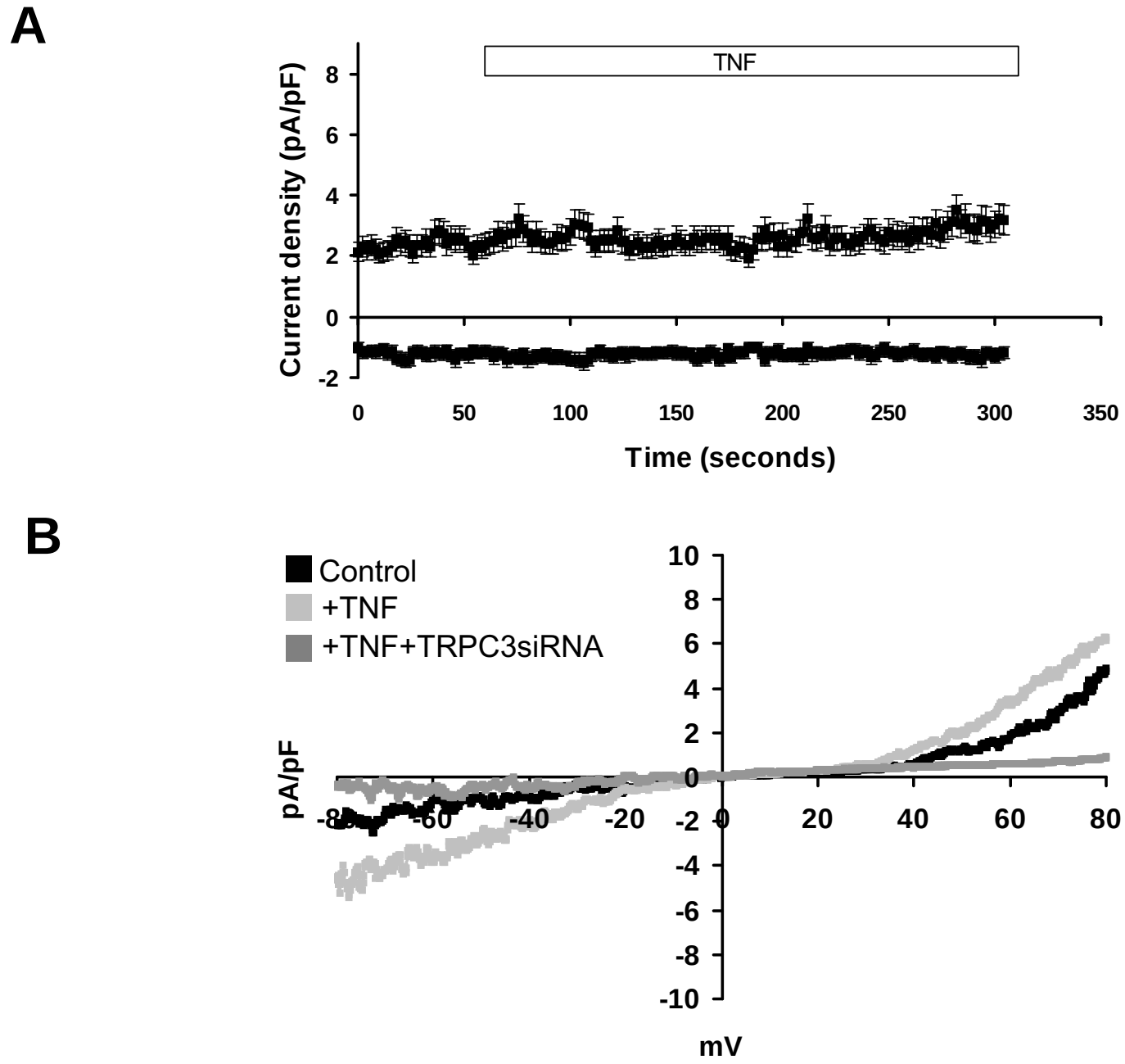
A
TNF
Current density (pA/pF)
8
6
4
2
0
-2
0
50
100
150
200
250
300
350
Time (seconds)
B
Control
+TNF
+TNF+TRPC3siRNA
pA/pF
10
8
6
4
2
0
-2
-4
-6
-8
-10
-80
-60
-40
-20
0
20
40
60
80
mV

Supplementary Figure III

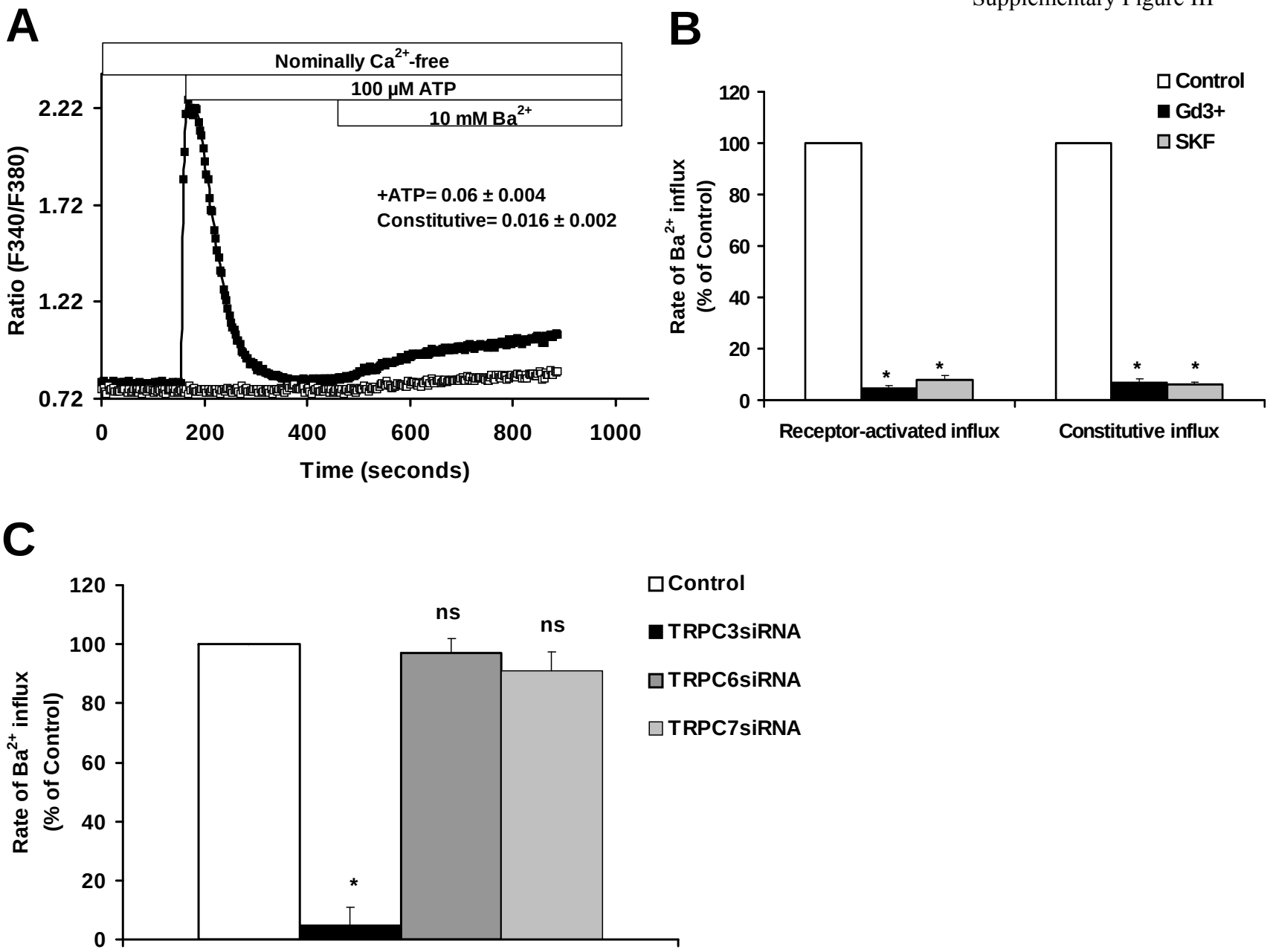

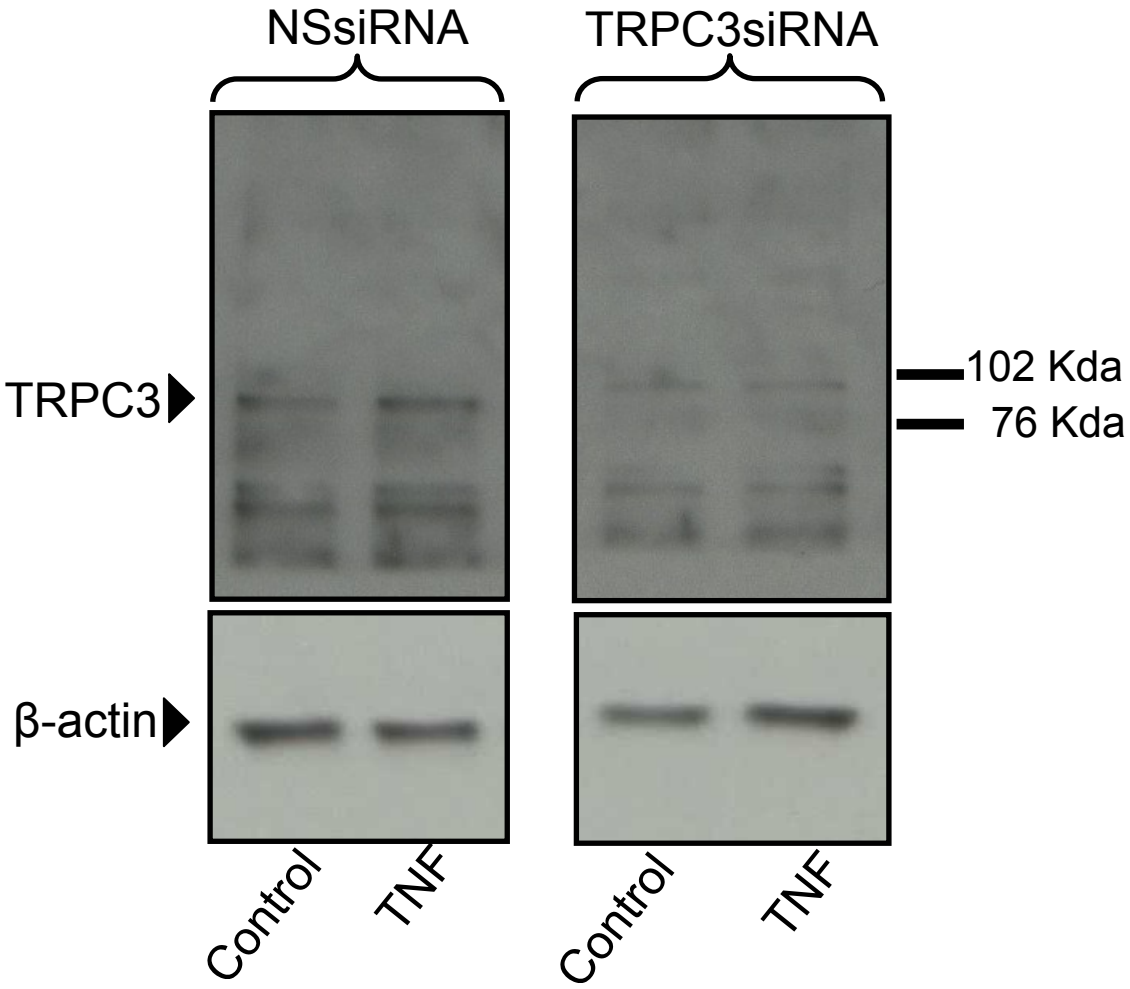
NSsiRNA
TRPC3siRNA
TRPC3
β-actin
102 Kda
76 Kda
Control
TNF
Control
TNF

Supplementary Figure V

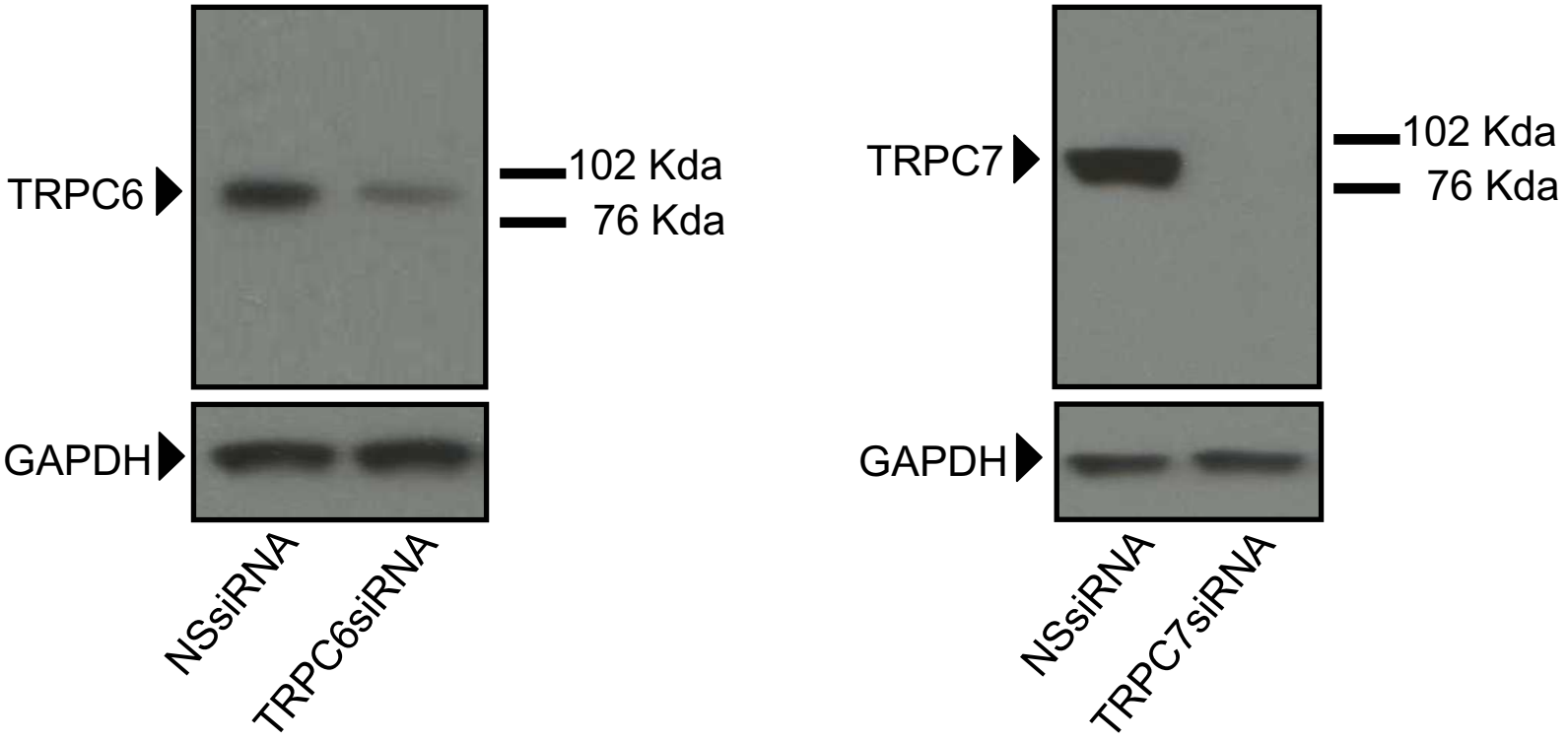

Supplementary Figure VI

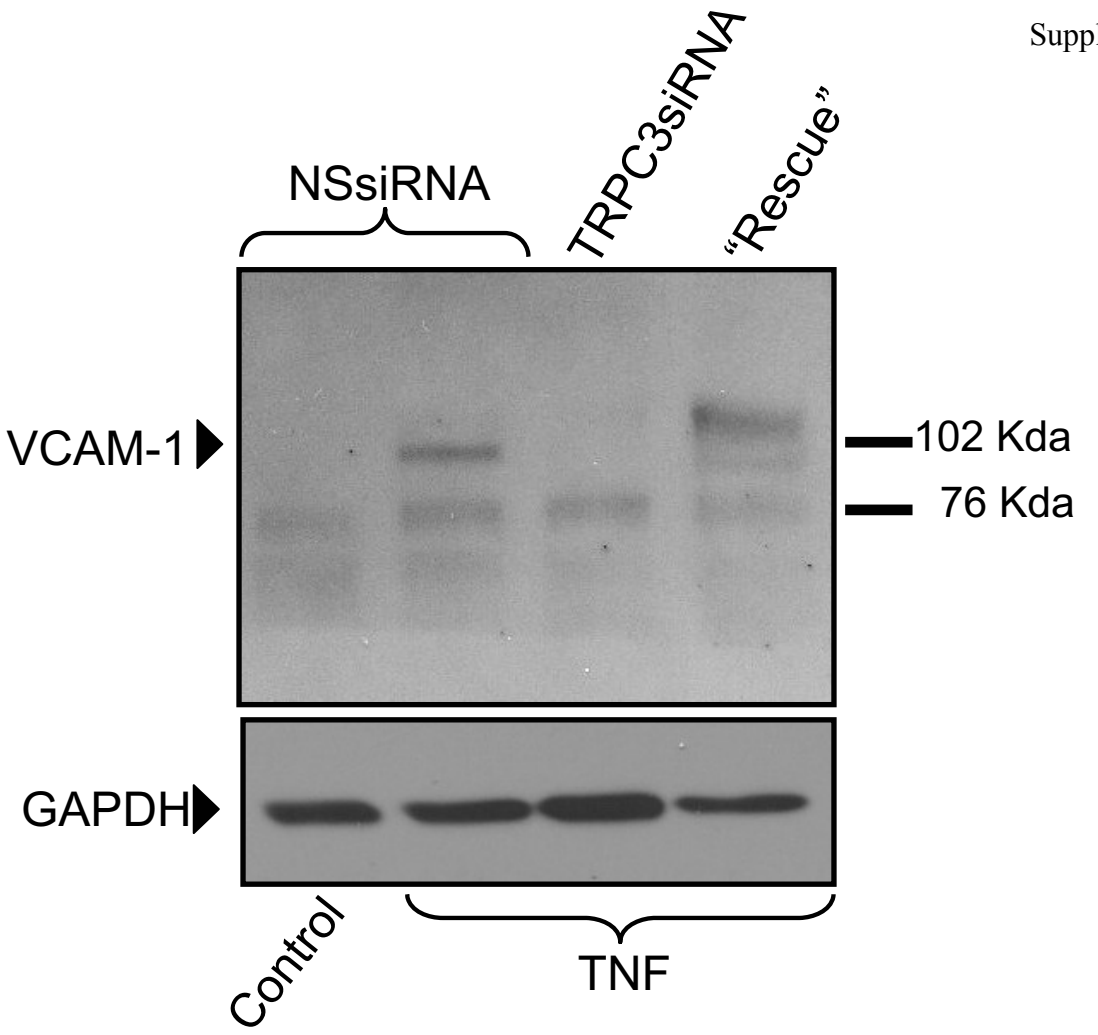

Supplementary Figure VII

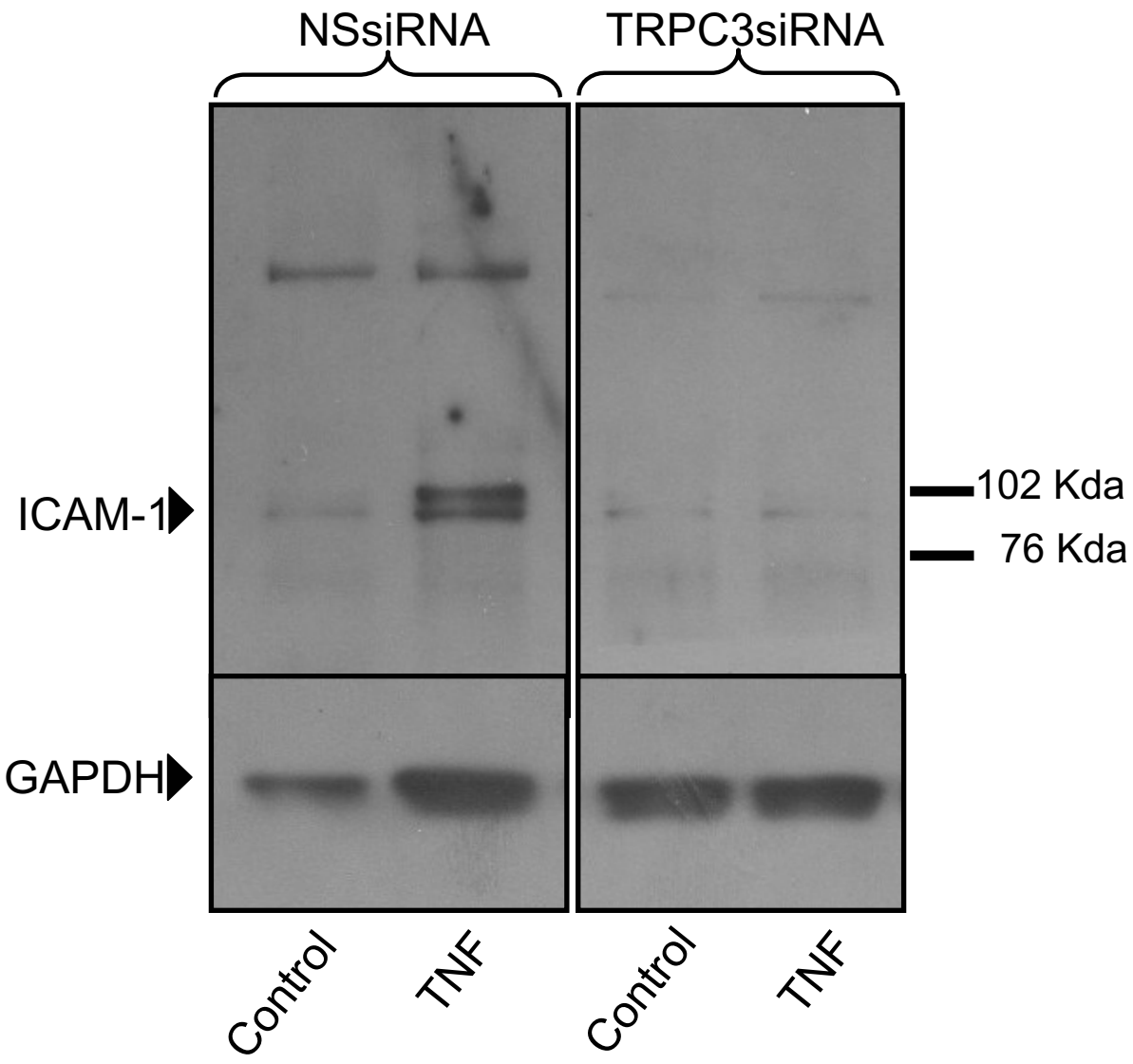

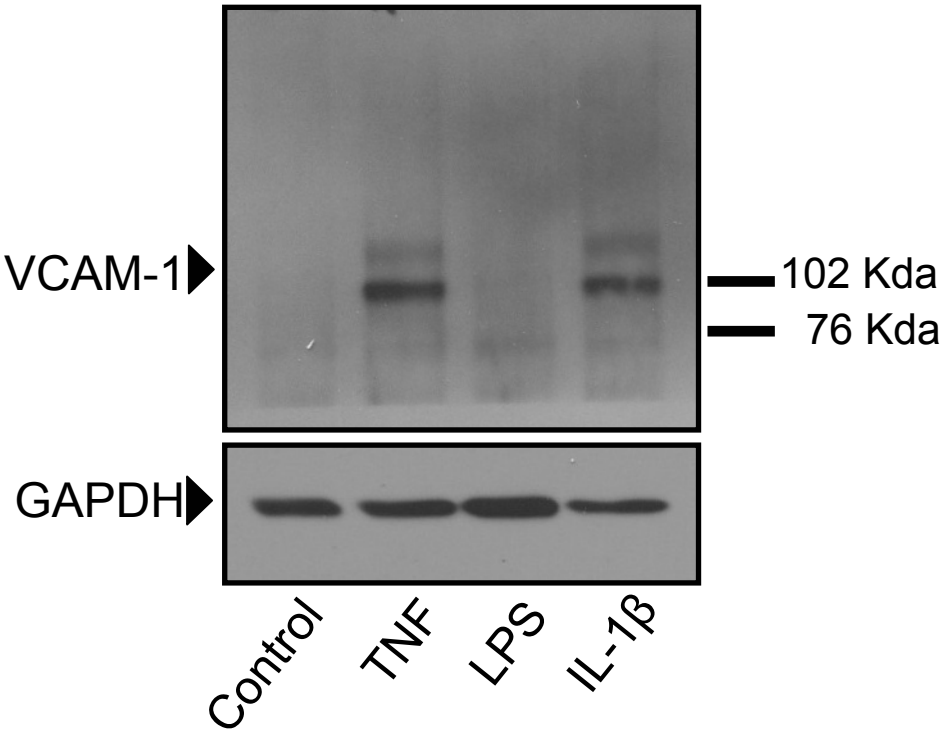

Supplementary Figure IX

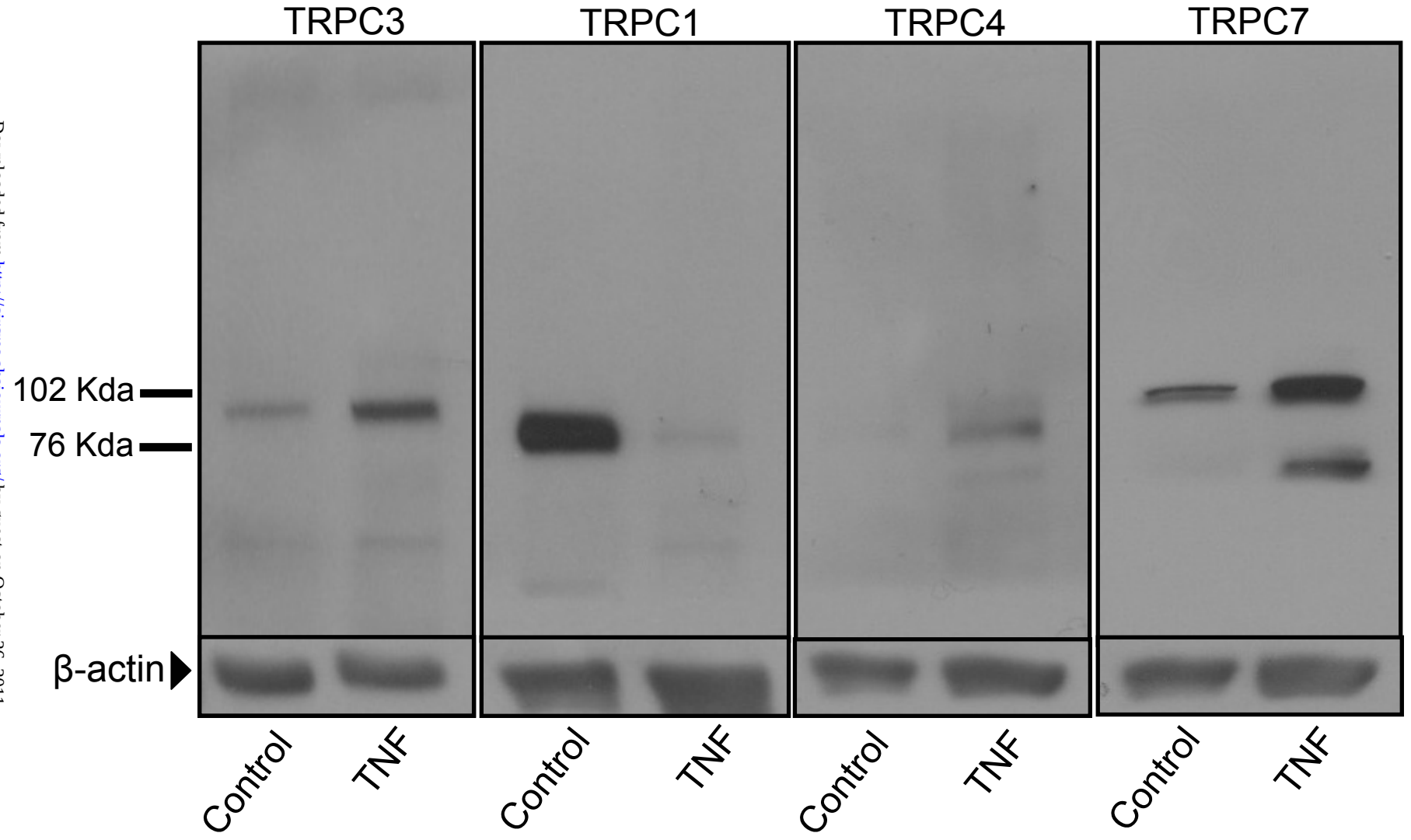

Supplementary Figure X

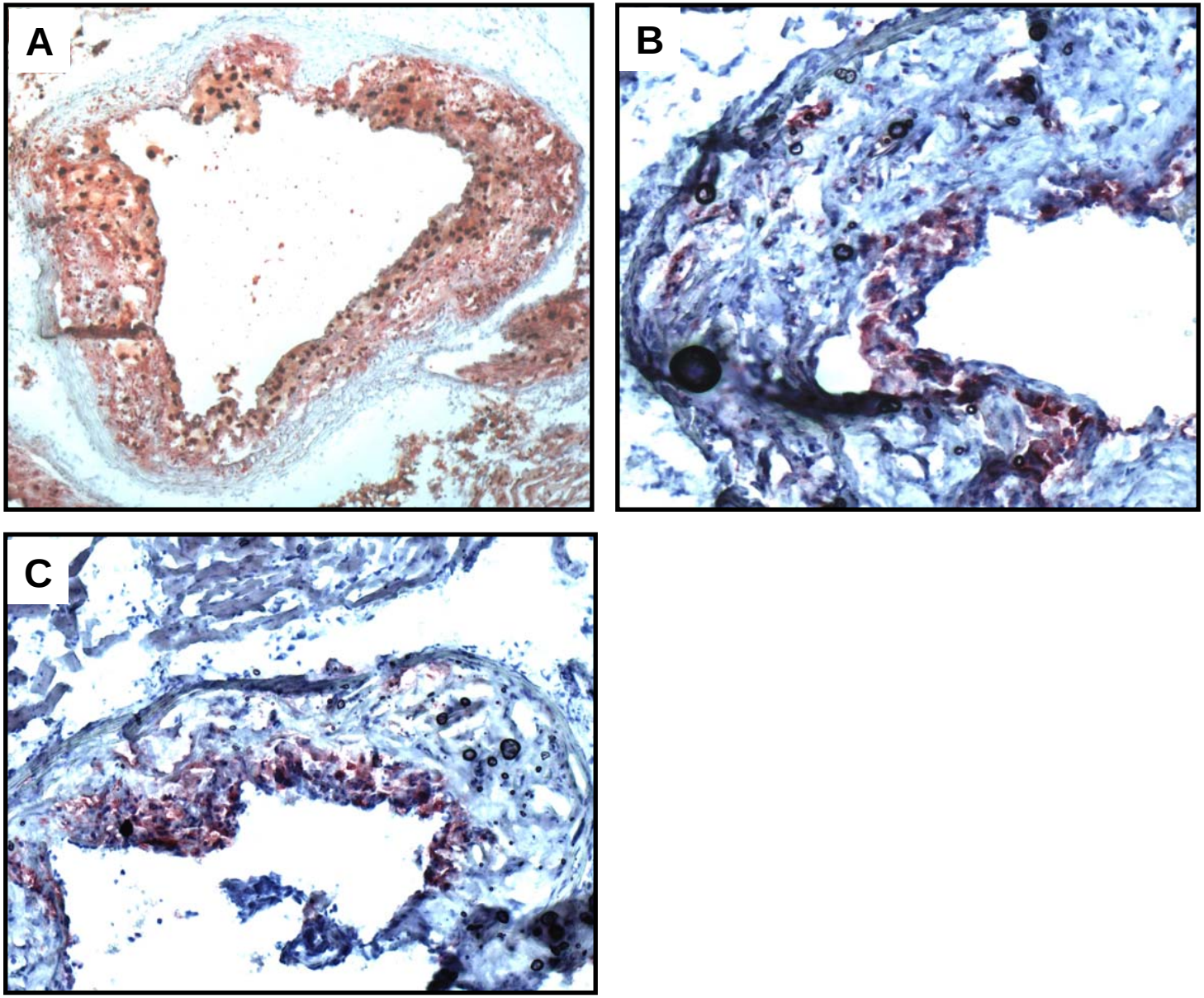

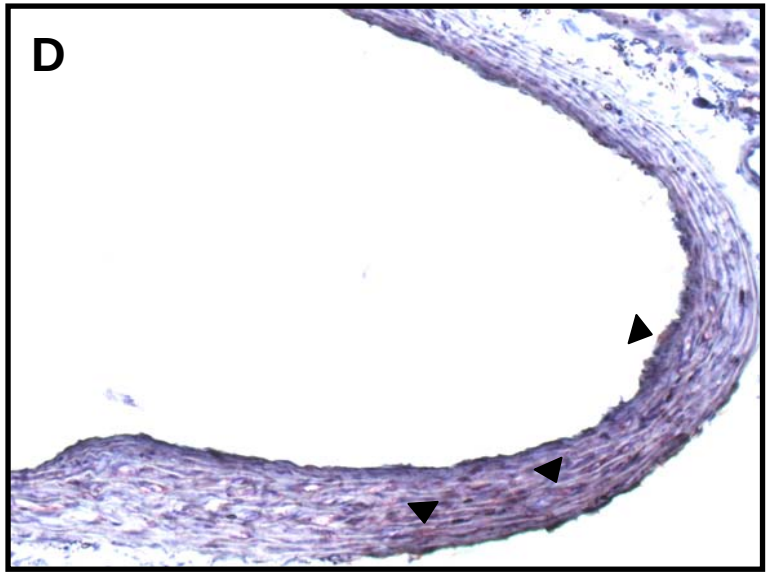

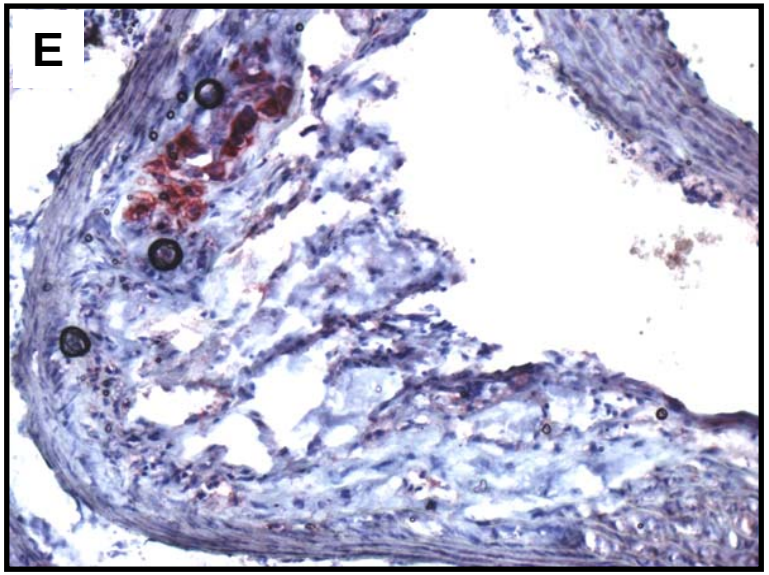

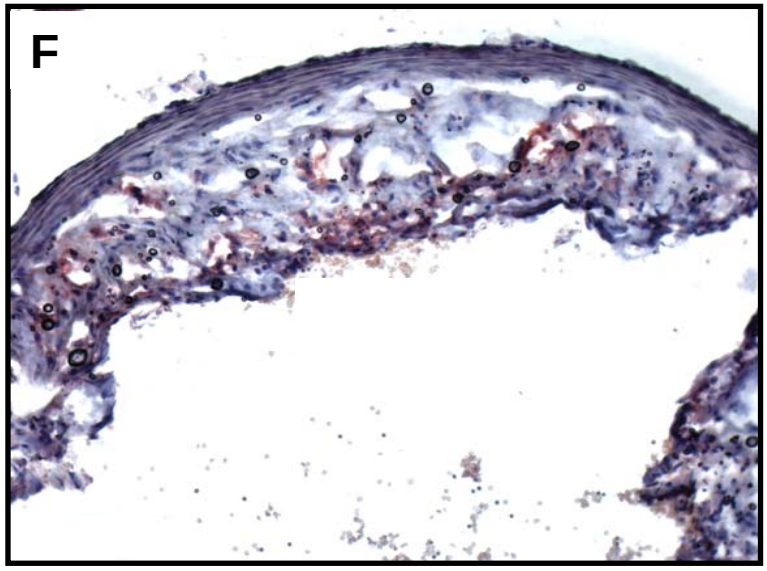

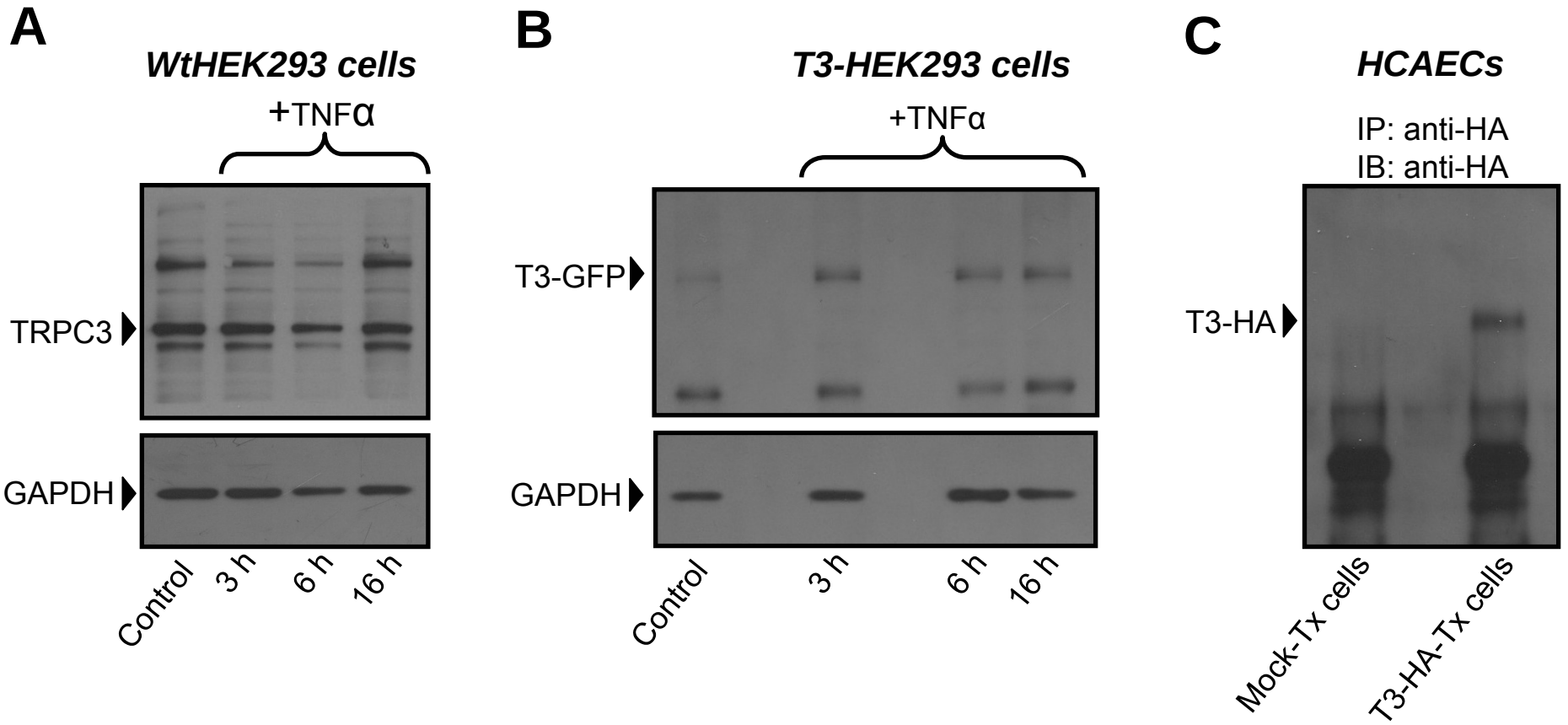
A
WtHEK293 cells
+TNFα
TRPC3
GAPDH
Control
3 h
6 h
16 h
B
T3-HEK293 cells
+TNFα
T3-GFP
GAPDH
Control
3 h
6 h
16 h
C
HCAECs
IP: anti-HA
IB: anti-HA
T3-HA
Mock-Tx cells
T3-HA-Tx cells

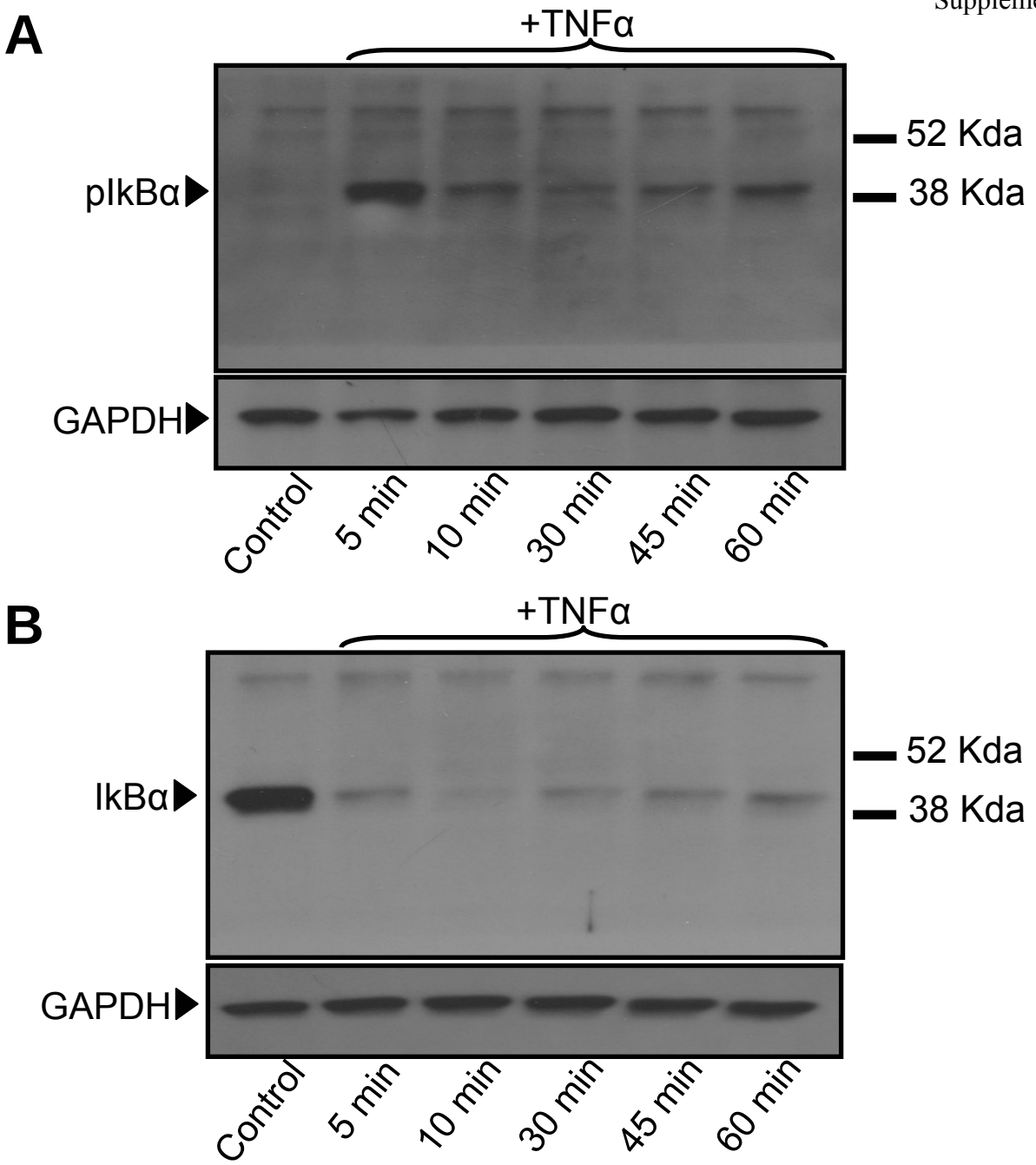
A
+TNFα
pIkBα
GAPDH
52 Kda
38 Kda
Control
5 min
10 min
30 min
45 min
60 min
B
+TNFα
IkBα
GAPDH
52 Kda
38 Kda
Control
5 min
10 min
30 min
45 min
60 min

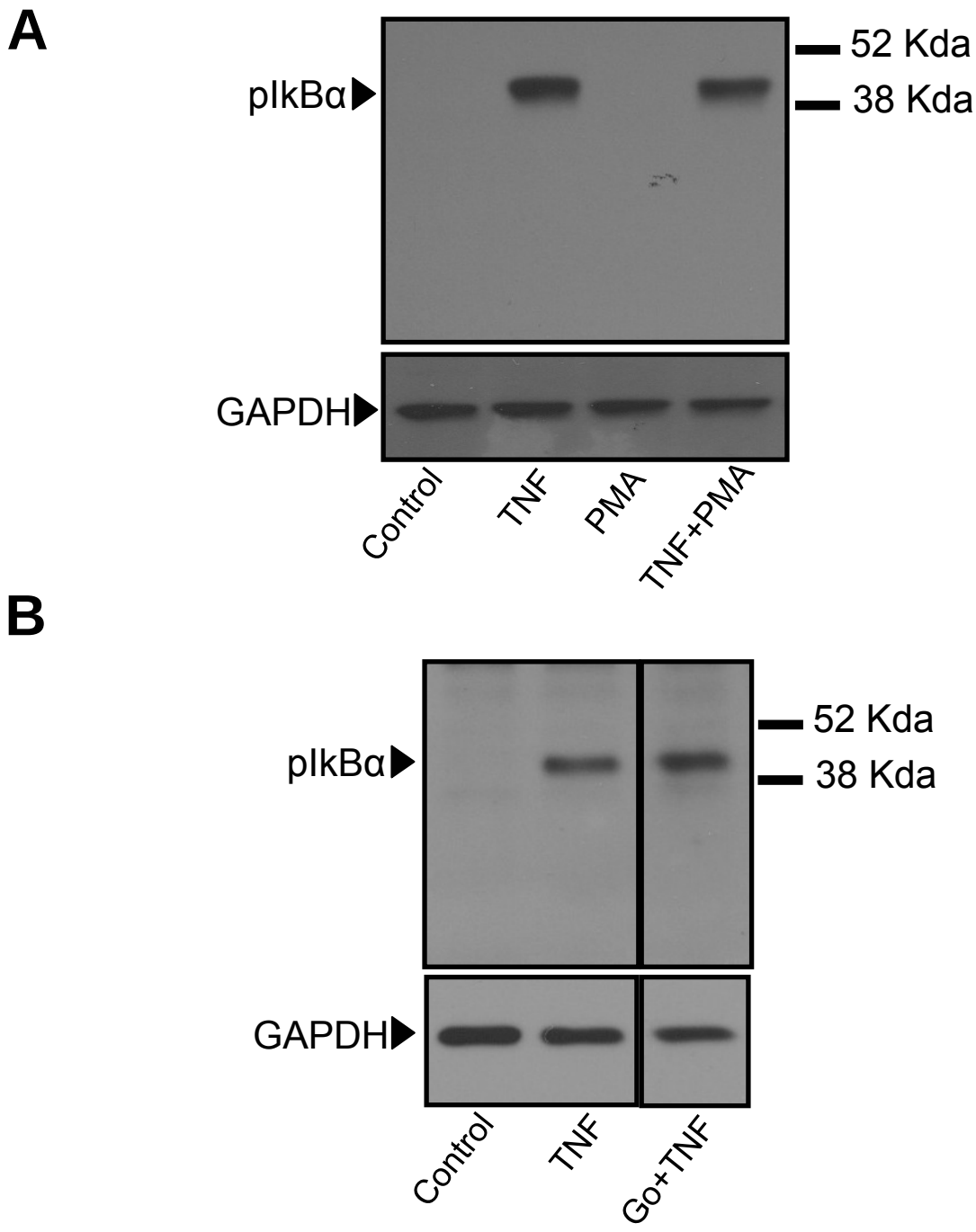
A
pIkBα
52 Kda
38 Kda
GAPDH
Control
TNF
PMA
TNF+PMA
B
pIkBα
52 Kda
38 Kda
GAPDH
Control
TNF
Go+TNF